Large-Amplitude Mesoscale Wave Disturbances Within the Intense Midwest Extratropical Cyclone of 15 December 1987

RUSSELL S. SCHNEIDER

Department of Meteorology, University of Wisconsin, Madison

(Manuscript received 15 December 1989, in final form 24 August 1990)

ABSTRACT

On 15 December 1987 several long-lived, large-amplitude mesoscale wave disturbances embedded within a rapidly intensifying extratropical cyclone traversed the Midwest and created life-threatening blizzard conditions. Within the wave disturbances, which likely were atmospheric gravity waves, pressure falls of up to 11 mb in 15 min were accompanied by winds in excess of 30 m s^{-1} (60 kt), cloud-to-ground lightning and heavy snowfall. One of the large-amplitude mesoscale wave disturbances, characterized by a surface pressure minimum lower than the cyclone's central pressure, propagated through the cyclone center during the rapid intensification stage of the storm system. The rapid changes in weather conditions associated with these wave disturbances played havoc with attempts to make short-range forecasts at the height of the 15 December 1987 snowstorm. To help forecasters anticipate and identify mesoscale wave disturbances, basic forecast guidelines based on gravity wave principles and recent research results are discussed.

1. Introduction

There is an increasing awareness of the existence and importance of atmospheric mesoscale wave disturbances with long duration ($\Delta t > 4$ h), long periods ($\tau > 1$ h), and large amplitudes ($p' > 2$ mb) by both operational and research meteorologists. Mesoscale wave disturbances are frequently identified as atmospheric gravity or inertia-gravity waves which can produce rapid variations in surface wind, pressure, visibility, cloud cover, and precipitation rate (Hooke 1986). The waves are also accompanied by strong vertical wind shear and severe turbulence that pose major hazards to air travel (Bosart and Seimon 1988). A climatology of surface pressure events during 33 winter seasons at Madison, Wisconsin revealed an average of one wave episode with a wave amplitude greater than 2 mb per winter month and an episode with a wave of amplitude greater than 3.5 mb once per winter season (Young and Richards 1973). Numerous cases of large-amplitude cold-season and warm-season wave episodes have been documented in the literature (summarized in Uccellini and Koch (1987) and Hooke (1986)). As such, mesoscale wave disturbances frequently create dangerous weather conditions and are a difficult but important problem for operational and research meteorologists.

The mesoscale wave disturbances accompanying the 14–15 December 1987 extratropical cyclone over the central United States were particularly intense. Pressure falls of up to 11 mb in 15 min were accompanied by heavy snow, ice pellets, cloud-to-ground lightning, and surface winds gusting to 30 m s^{-1}. The combined effect of wind and heavy snow created blizzard conditions over much of northern Illinois and southeast Wisconsin. The wave disturbances were closely associated with the rapid intensification period of the parent extratropical cyclone, during which the cyclone's minimum mean-sea-level pressure decreased 20 mb in 12 h. For several hours, the minimum surface pressure associated with the wave disturbances was lower than the central pressure of the parent extratropical cyclone. The rapid changes in weather conditions associated with the wave disturbances made their detection and understanding essential to a successful short-range forecast on 15 December 1987.

The purpose of this article is to document the meteorological conditions that accompanied the large-amplitude mesoscale wave disturbances, and to highlight the impact of these waves on the attempts by forecasters to monitor and forecast the rapidly changing conditions. A complete quantitative analysis of the wave disturbances similar to Stobie et al. (1983) or Koch and Golus (1988) is not attempted. Section 2 provides a synopsis of the large-scale atmospheric conditions. Section 3 compares key observations with gravity wave theory and details the analysis procedure used to isolate the wave disturbances. Section 4 describes wave interaction with the extratropical cyclone and the abrupt changes in weather which accompanied wave disturbance passage. In section 5, the impact of the waves on the operational weather forecast/nowcast is described. Section 6 applies gravity wave theory to facilitate understanding of the processes responsible for wave formation, intensification, and maintenance; and section 7 provides some simple guidelines for predic-

Corresponding author address: Russell S. Schneider, Dept. of Meteorology, University of Wisconsin, 1225 West Dayton Street, Madison, WI 53706.

tion and detection of wave events. Finally, section 8 summarizes important characteristics and scientific questions raised by the 15 December 1987 wave disturbances.

2. Large-scale conditions

On 13 and 14 December 1987, a large-scale upper-level trough was located over the western United States with broad southwesterly flow over the eastern two-thirds of the country. A strong short-wave trough and associated 300-mb jet streak of 65 m s^{-1} near Baja, California propagated through the base of the upper-level trough over the western United States, and within 24 hours, surface cyclogenesis began in southeast Texas.

By 0000 UTC 15 December, the surface cyclone was located in south-central Arkansas (Fig. 1a) and was about to begin a 12-h period of rapid intensification as strong cyclonic vorticity advection associated with the upstream upper-level trough overspread the surface cyclone center (Fig. 1b). Between 0000 UTC and 1200 UTC 15 December, the storm moved rapidly northeastward to northeast Illinois and the minimum mean-sea-level pressure decreased from 999 mb to 979 mb. The intense, negatively tilted, upper-level trough was nearly collocated with the surface cyclone center by 1200 UTC 15 December (Figs. 1c,d). Thereafter the occluded cyclone slowly decreased in intensity as it drifted northeastward into Michigan. In its wake, the cyclone left 15 to 40 cm (6 to 16 inches) of new snow in a 300-km wide band from the Texas panhandle to Northern Michigan (Fig. 2). Although the snowfall amounts within this band were relatively uniform, the mesoscale wave disturbances accompanying the cy-

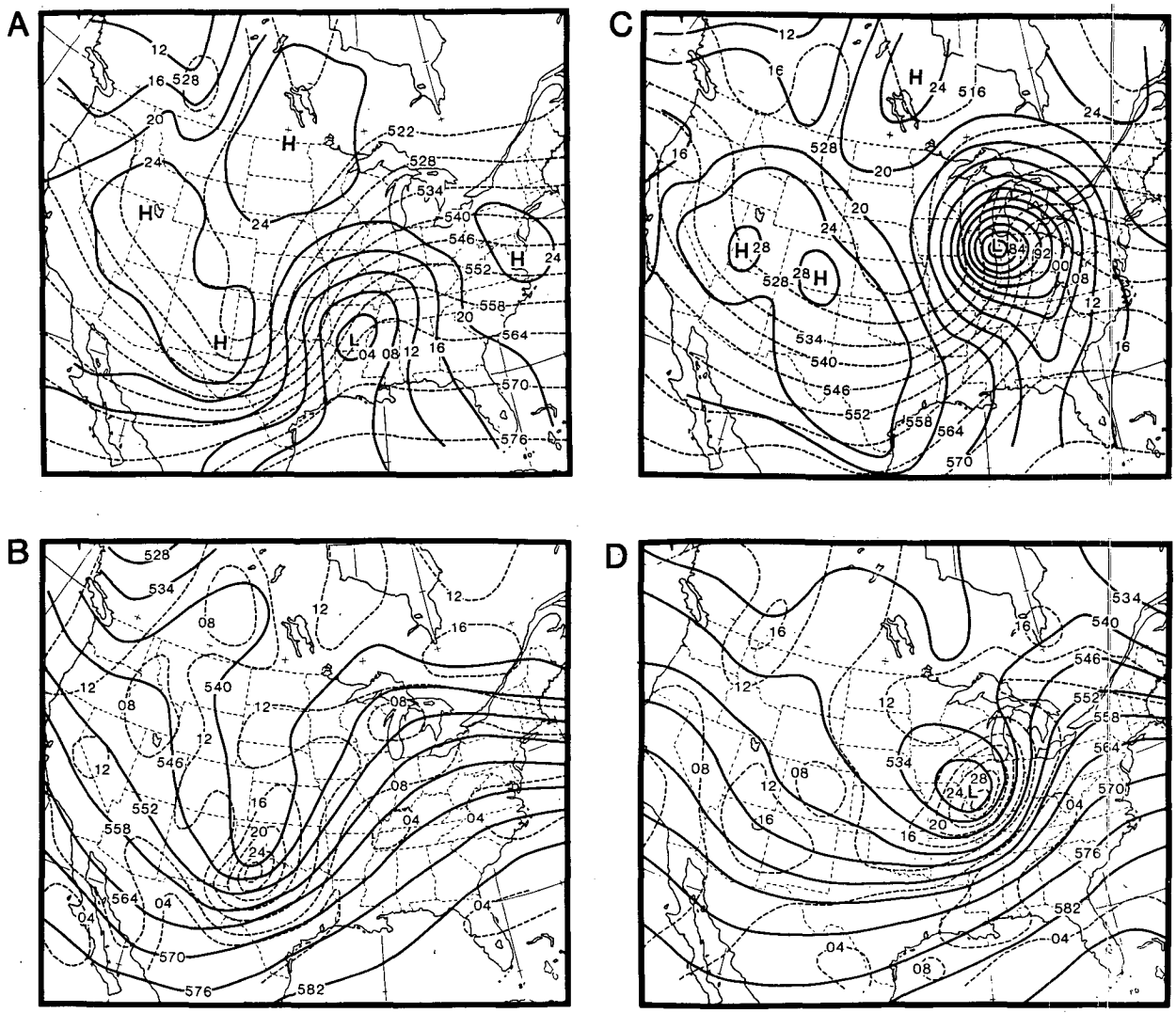

FIG. 1. Subjective analyses of: (A) mean-sea-level pressure (solid; contoured every 4 mb) and 1000–500-mb thickness (dashed; contoured every 6 dam) and (B) 500-mb heights (solid; contoured every 6 dam) and absolute vorticity (dashed; contoured every $4 \cdot 10^{-5}$ s^{-1}) for 0000 UTC 15 December 1987. (C) and (D) are the same as (A) and (B) but for 1200 UTC 15 December 1987.

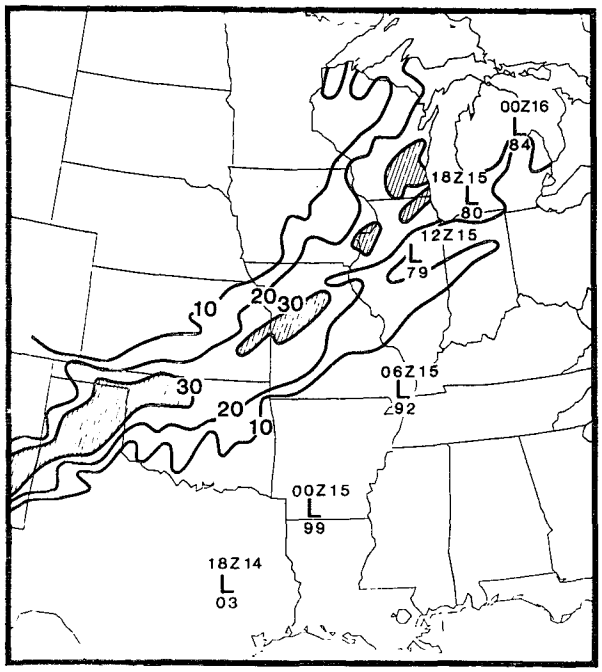

FIG. 2. Snowfall (cm) on 13–16 December 1987. Stipled area experienced snowfall greater than 30 cm (12 in.). Positions of the cyclone center based on NMC and subjective analyses (denoted by '*L*') and central mean-sea-level pressure (mb; leading '9' or '10' omitted) are also plotted.

clone created rapid fluctuations in local weather conditions which dramatically increased the rate and impact of the heavy snowfall over periods of several hours.

3. Wave disturbance detection and analysis

In this section, a basic theoretical model of the structure and dynamics of atmospheric gravity waves is described, and dramatic Midwest observations from 15 December 1987 which were consistent with this model are presented. After a brief overview of the observed wave-troughs, details of their analysis using surface and satellite data are presented and the surface structure and temporal evolution of the wave disturbances are described.

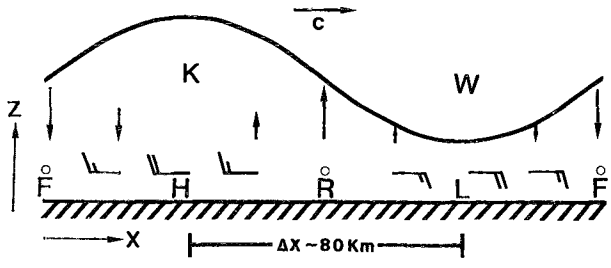

FIG. 3. Idealized vertical cross section of a linear plane gravity wave, with no basic current, propagating toward the right at speed *c*. The heavy sinusoidal line is a representative isentropic surface or a temperature inversion. Surface pressure extrema are labeled *H* and *L*, pressure rise and fall extrema by *R* and *F*, and mid-level cold and warm temperature anomalies are denoted *K* and *W* respectively (Adapted from Bosart and Sanders 1986).

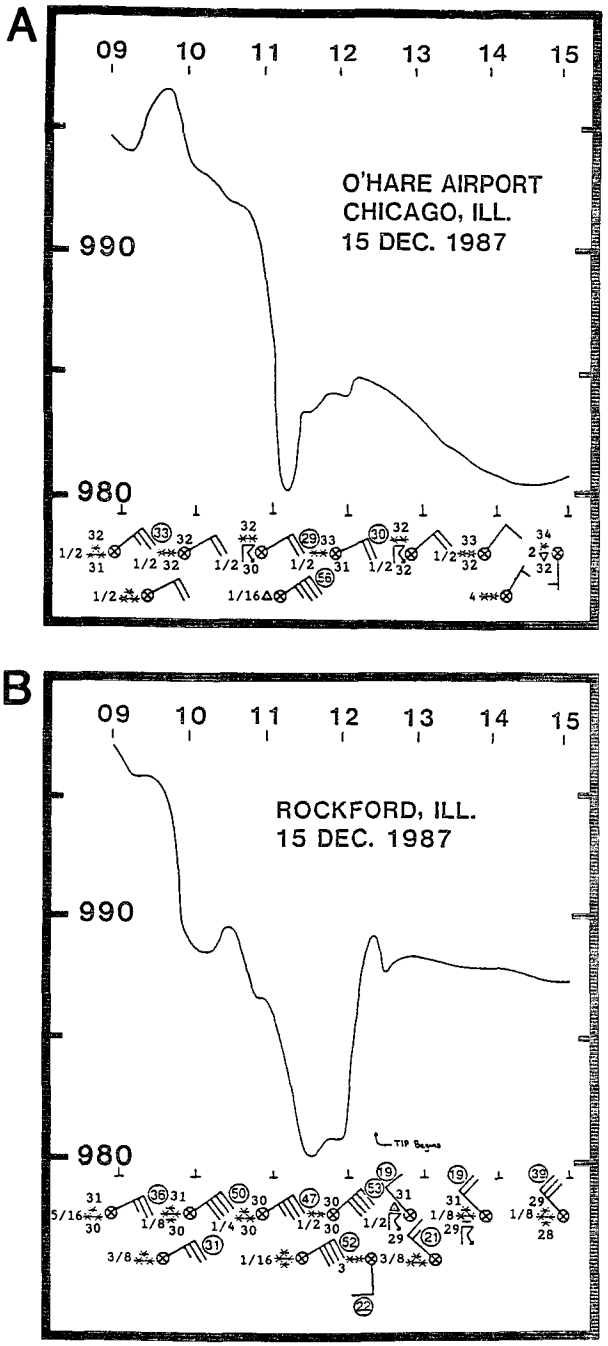

FIG. 4. Time series (UTC) of surface pressure and key surface observations at (A) O'Hare International Airport (ORD), Chicago, Illinois and (B) Rockford, Illinois (RFD) on 15 December 1987. Station plot includes wind (1 barb = 10 kt), wind gusts (near the end of the wind flag; kt), current weather, visibility (left of weather symbols, mi), and when available, temperature and dewpoint (above and below the location for weather symbols, °F). The onset time of a thunder and ice pellet shower is also indicated (TIP begins).

a. Comparison of theory and observations

Eom (1975) used a linear, two-layer, two-dimensional theoretical model to develop a schematic describing the structure of a simple atmospheric gravity

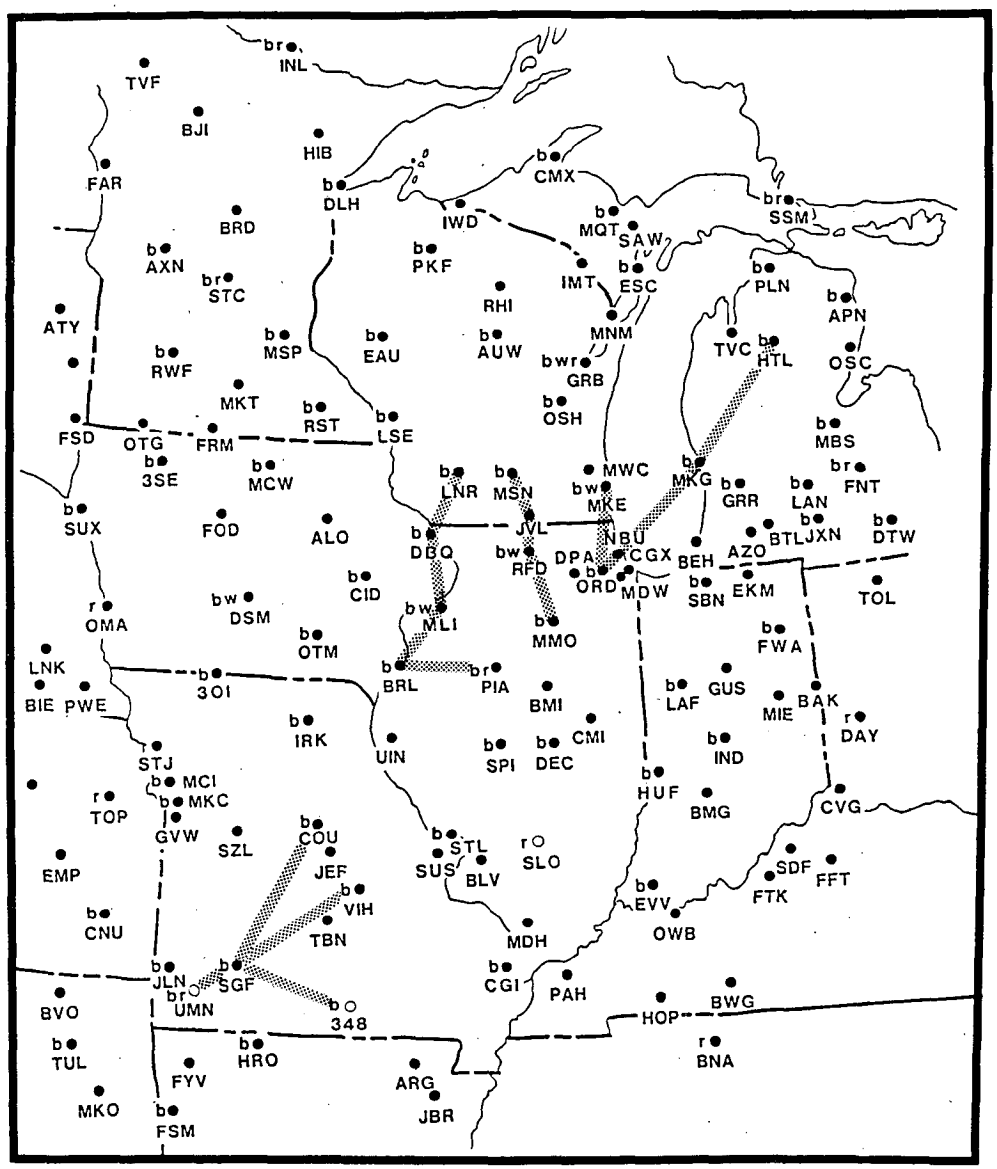

FIG. 5. Location and three-letter abbreviation for stations used in this study. Stations which report surface airways observations (SA) are denoted with a solid circle. Lower-case letters to the left of each station indicate barograph (*b*), rawinsonde (*r*), or wind recorder (*w*) data which was acquired for 0000 UTC–1800 UTC 15 December, 1987. Several low-order stations which report only sporadically are omitted from the map. The stations included in Fig. 6 are connected by stippled lines.

wave which propagates faster than the mean wind in the layer in which it is embedded (Fig. 3; adapted from Bosart and Sanders 1986). Strongest perturbation wind speeds coincide with high and low pressure perturbations (H and L in Fig. 3). To determine the total wind relative to the ground, the perturbation winds are added to the mean wind in the layer that the wave is traveling through. Maximum ascent and descent coincide with the strongest low-level convergence and divergence which are also collocated with the largest surface pressure rises (*R*) and falls (*F*). The greatest vertical displacement of a parcel passing through the wave is attained after passage of the band of strong upward vertical motion and is coincident with the maximum positive perturbation pressure (*H*). The upward vertical motion creates the anomalously cold mid-level air (*K*) associated with the pressure ridge through upward displacement of a low-level stable layer. The converse occurs in the region of subsidence preceding the pressure trough.

The largest precipitation rate and deep cloudiness associated with this idealized wave are expected between the upward vertical motion maximum (collocated with *R*) and the trailing wave ridge axis (*H*). Many observational studies support this model (Eom 1975; Uccellini 1975; Stobie et al. 1983; Pecnick and

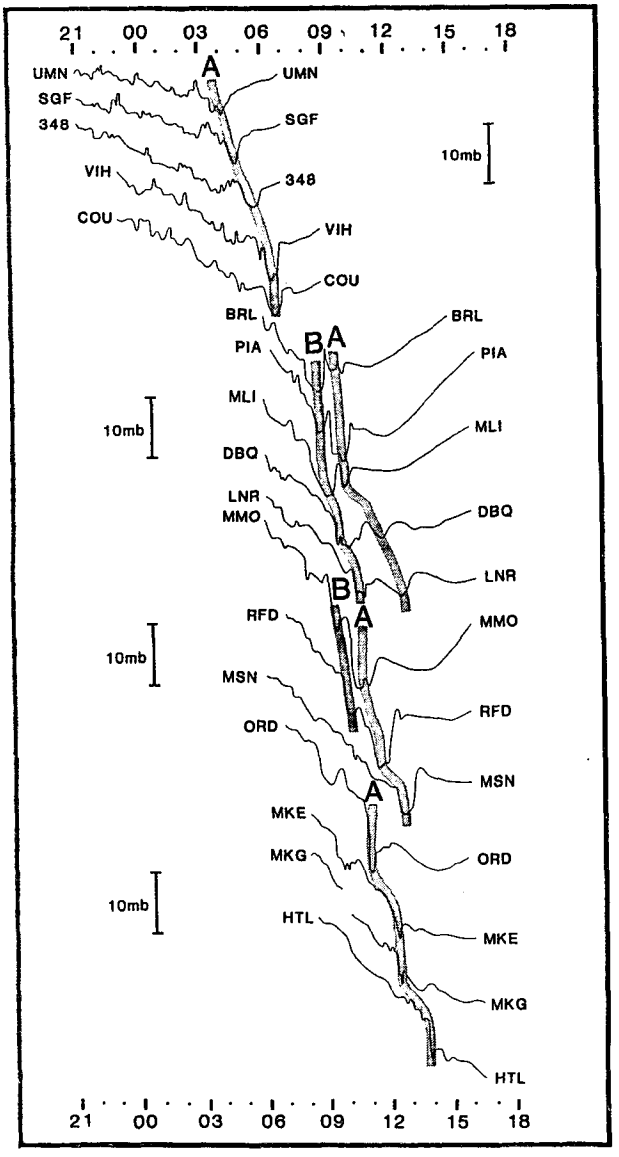

FIG. 6. Graphs of surface pressure (mb) as a function of time (UTC) from stations across the Midwest between 2100 UTC 14 December and 1800 UTC 15 December 1987 which highlight rapid, large-amplitude pressure fluctuations associated with mesoscale wave-troughs A and B. The pressure minima associated with these wave-troughs are connected by stippled line segments.

Young 1984; Bosart and Sanders 1986; Koch et al. 1988). In two of these large-amplitude gravity wave events, only enhanced cloudiness or light precipitation occurred with wave passage (Eom 1975; Pecnick and Young 1984). Koch and Golus (1988) note that if the wave tilts upstream with height, as documented in a case study by Pecnick and Young (1984), the maximum precipitation rate can occur during, or even slightly after ridge axis passage.

Other complications to this simplified gravity wave model have been observed. In several studies of gravity waves characterized by a single negative pressure perturbation not accompanied by a trailing positive pressure perturbation, subsidence ahead of the pressure minimum is associated with the dissipation of mid-level clouds and the end of an extended period of precipitation (Tepper 1951; Bosart and Cussen 1973; Bosart and Seimon 1988). Thus the evolution of precipitation accompanying observed wave disturbances can differ significantly from the idealized gravity wave model depending on the environmental stability, water vapor content, and the actual vertical structure of the wave.

For the 15 December 1987 case, surface observations at Rockford, Illinois and at O'Hare International Airport in Chicago, Illinois illustrate the intensity of the mesoscale wave disturbances and their agreement with gravity wave theory (Fig. 4). In particular, the occurrence of relative maxima in surface wind speeds coincident with abrupt local minima in surface pressure at both O'Hare (1106 UTC) and Rockford (1000 UTC and 1130 UTC) are characteristic of the passage of an atmospheric gravity wave (compare Figs. 3, 4). In contrast to passage of the mesoscale wave disturbances, light winds accompanied passage of the surface cyclone pressure minimum at O'Hare (1430 UTC) (Fig. 4a). The dramatic wind shift near the end of the rapid pressure rise at Rockford, Illinois (1200–1225 UTC) followed by the onset of heavy convective snowfall is also consistent with an idealized gravity wave with upstream tilt embedded in large-scale, low-level northeasterly flow. Passage of a classic convectively generated mesoscale high pressure system is characterized by a strong wind shift near the onset of the rapid pressure rise and is frequently accompanied by a significant decrease in surface temperature (Fujita 1955; Doswell 1982). At Rockford, the wind did not shift direction until 20 min after the rapid pressure rise began and the temperature remained nearly constant throughout the rapid pressure oscillations.

Surface barograms from across the Midwest (Figs. 5, 6) revealed similar high-frequency pressure oscillations characteristic of atmospheric gravity waves. At most stations, numerous pressure oscillations of 0.2 mb to 3 mb preceded passage of one or two additional oscillations with amplitudes greater than 4 mb. Within the two hours surrounding the passage of the major pressure disturbances, only one of 25 affected stations reported a 1-h surface temperature or dewpoint change greater than 1°F (UIN, 2°F in 1 h). A northeastward progression of the abrupt, large-amplitude pressure minima observed at Rockford and O'Hare is suggested by the selected barograms in Fig. 6 which are arranged by location generally from southwest (Monett, Missouri (UMN)) through northeast (Houghton Lake, Michigan (HTL)) and subdivided to facilitate comparison of western and eastern segments of the major wave troughs (Fig. 5). These large-amplitude pressure troughs are the focus of this investigation.

b. Overview

Two major mesoscale pressure troughs were isolated using surface observations, satellite imagery, and guid-

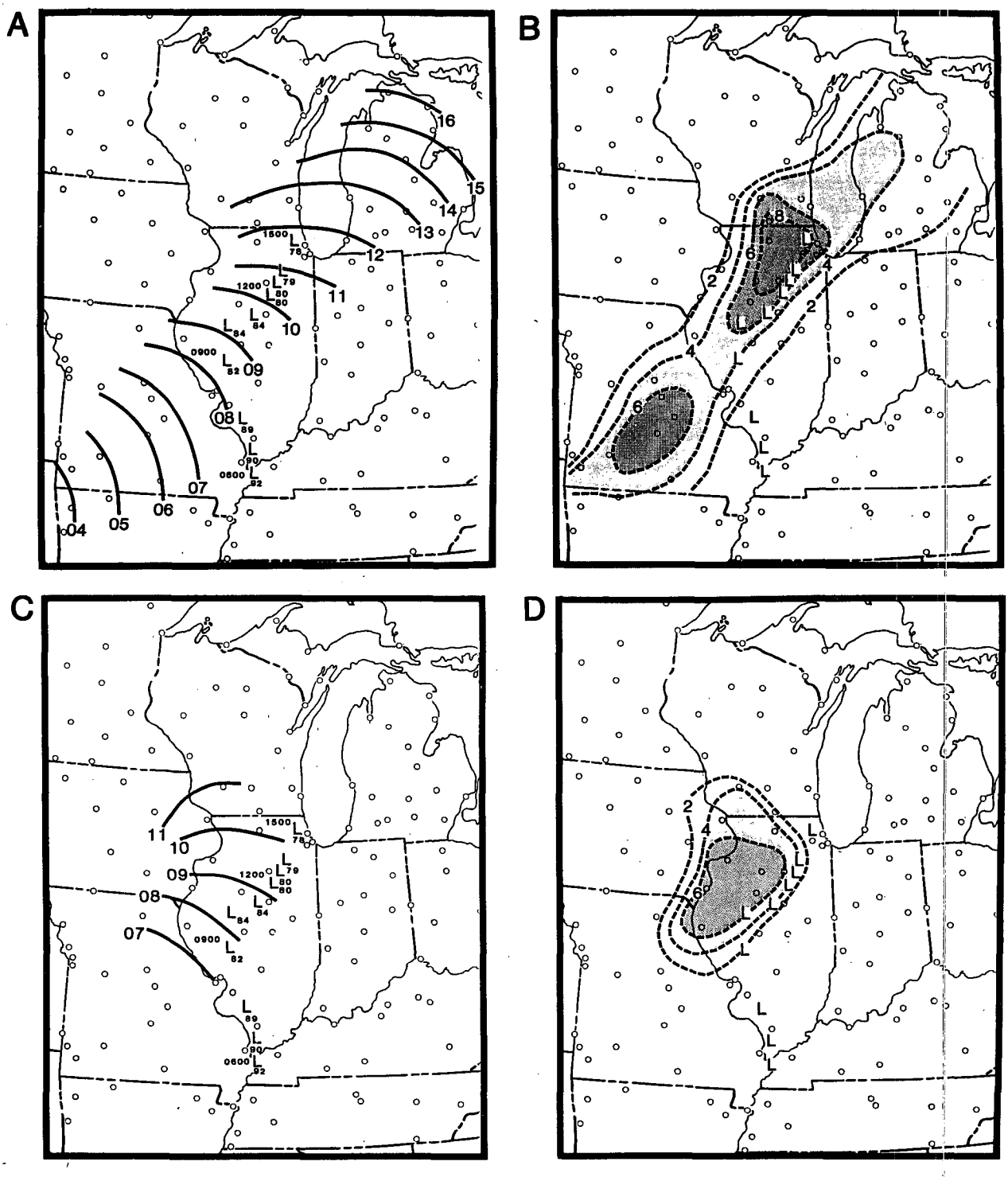

FIG. 7. (A) Isochrones of the location of wave-trough A (solid, UTC) on 15 December 1987. The position of the extratropical cyclone ('*L*'), the minimum sea-level pressure (below '*L*'; mb; lead '9' or '10' omitted), and the time at 3-h intervals (above and left of '*L*'; UTC) are plotted. To match synoptic observations, the position of each isochrone is the estimated wave location 10 min before the labeled hour. (B) Peak-to-peak amplitude of wave-trough A (dashed, mb) (see text for definition). (C) and (D) are the same (A) and (B) except the data is for wave-trough B.

ance from gravity wave theory. Designated wave-trough A and wave-trough B, these pressure troughs were confined to an envelope roughly 400 km wide extending northeastward from southwest Missouri to Michigan (Figs. 7a,c). The pressure minimum associated with wave-trough A was first evident in surface observations

at Monett, Missouri (UMN) and Fayetteville, Arkansas (FYV) at approximately 0400 UTC 15 December (Figs. 5, 6). Although numerous small-amplitude pressure perturbations ($p' < 2$ mb) were observed at upstream stations in Oklahoma, a large-amplitude pressure trough similar to wave-trough A was not detected prior to 0330 UTC. The origin of wave-trough B was more difficult to determine and required consideration of the temporal evolution of wave-trough A, as will be discussed shortly.

Both wave-troughs moved north-northeastward at 30 m s^{-1} (discussed in section 6b) with average peak-to-peak amplitudes of approximately 6 mb (Figs. 7b,d). The peak-to-peak amplitudes of the waves (hereafter referred to as the amplitude) were computed by summing the observed pressure fall and rise with wave trough passage and dividing by two. This methodology provided a conservative estimate of the wave amplitude by subjectively removing a linear pressure tendency associated with synoptic-scale pressure changes. Wave-trough A, the strongest of the wave disturbances, had a maximum amplitude of 9.6 mb (Fig. 7b). This was smaller than the 14-mb amplitude reported by Bosart and Seimon (1988) in a gravity wave over the southeast United States on 27 February 1984. The maximum observed amplitude of wave-trough B was 7.6 mb.

c. Analysis with surface and satellite data

The presence of mesoscale wave disturbances within the 15 December 1987 cyclone was strongly suggested by abrupt changes in surface pressure, wind, and weather conditions observed at stations throughout the Midwest. Despite their large amplitude, analysis of wave disturbance structure, evolution, and dynamics was complicated by the sparse, sometimes poor quality barogram traces, closure of key surface observation stations at night, and the coarse temporal and spatial resolution of existing surface airways (SA) observations. The sparse data network was particularly deficient between 0700 UTC and 0900 UTC when the wave disturbance activity was located near the Missouri–Illinois border. Therefore, estimates of wave-trough locations based on available surface barograms and SAs throughout the Midwest (Fig. 5) were refined using computer animated, rapid-scan, infrared (IR) satellite imagery on McIDAS (Suomi et al. 1983).

The mesoscale spatial and temporal resolution of rapid-scan IR satellite imagery was exploited to establish a relationship between observed cloud structures and the location of mesoscale surface pressure maxima and minima in surface barogram traces. Recall that linear gravity wave theory (Fig. 3) suggests that pressure maxima associated with mesoscale wave disturbances can induce the development of deep cloud bands characterized by cold infrared temperatures (bright bands). Pressure minima are associated with shallow clouds or cloud-free bands characterized by warm infrared temperatures (dark bands). In practice, slight adjustments to this model were required due to apparent variations in the vertical tilt of the wave disturbances (similar to Pecnick and Young 1984) suggested through comparison of the barogram and satellite data. Then the spatial and temporal evolution of cloud structures were used to guide construction of hourly surface analyses of the altimeter setting and major wave disturbance trough and ridge axes.

Altimeter settings, rather than mean-sea-level pressure, were used in all surface analyses except Figs. 1b and d in order to maximize the size of the data base. When little ambiguity is introduced, the terms "altimeter setting" and "surface pressure" are used interchangeably. Small-scale structures in the wave disturbances were smoothed out in the surface analyses, and at some stages in the evolution of the disturbances, observation of a 40-km wide pressure minimum made assignment of a specific line to the trough location subjective.

Select infrared (IR) satellite imagery from GOES-East (Fig. 8) and 3-hourly surface analyses (Fig. 9) provided an overview of the wave activity. The evolution of the large-scale cloud shield into the large-scale comma shape often associated with intense extratropical cyclones (e.g., Carlson 1980) was evident in the image sequence (Fig. 8). Throughout their lifecycles, the large-amplitude mesoscale wave disturbances (dashed lines in Fig. 8) were closely associated with a smaller-scale comma cloud evident over central Missouri at 0546 UTC (Fig. 8c). At 0000 UTC, this small-scale comma cloud was associated with the north–south cloud band (*P*) over east-central Oklahoma and northern Texas (Fig. 8a), and collocated with intense 500-mb cyclonic vorticity advection and implied upper-level divergence ahead of a strong shortwave trough and jet streak (compare Figs. 1a, 8a).

During the 6 h from 0000 UTC to 0600 UTC, the north–south cloud band (P) moved east-northeastward into Missouri and contracted in width as it evolved into the comma-cloud shape associated with positive vorticity advection (Anderson 1974) (Figs. 8a,b,c). At 0546 UTC, mesoscale pressure ridges (dotted lines in Fig. 8c) were associated with the tail of the comma cloud which curved southward across central Missouri and the east–west cloud band over northeast Missouri. Wave-trough A (dashed line) was collocated with the warm IR blackbody temperature (dark) ribbon that trailed the central Missouri comma cloud.

The association between the ribbon of warm IR temperatures along the back edge of the small-scale comma cloud and wave-trough A was confirmed at each station within the relatively dense observing network over Missouri between 0400 UTC and 0700 UTC and suggests the presence of deep tropospheric subsidence ahead of the pressure minimum consistent with gravity wave theory (Pecnick and Young 1984). As wave-trough A traversed Missouri (0400 UTC–0700 UTC), the maximum IR temperatures within the warm band were collocated with the maximum peak-to-peak amplitude along the axis of wave-trough A

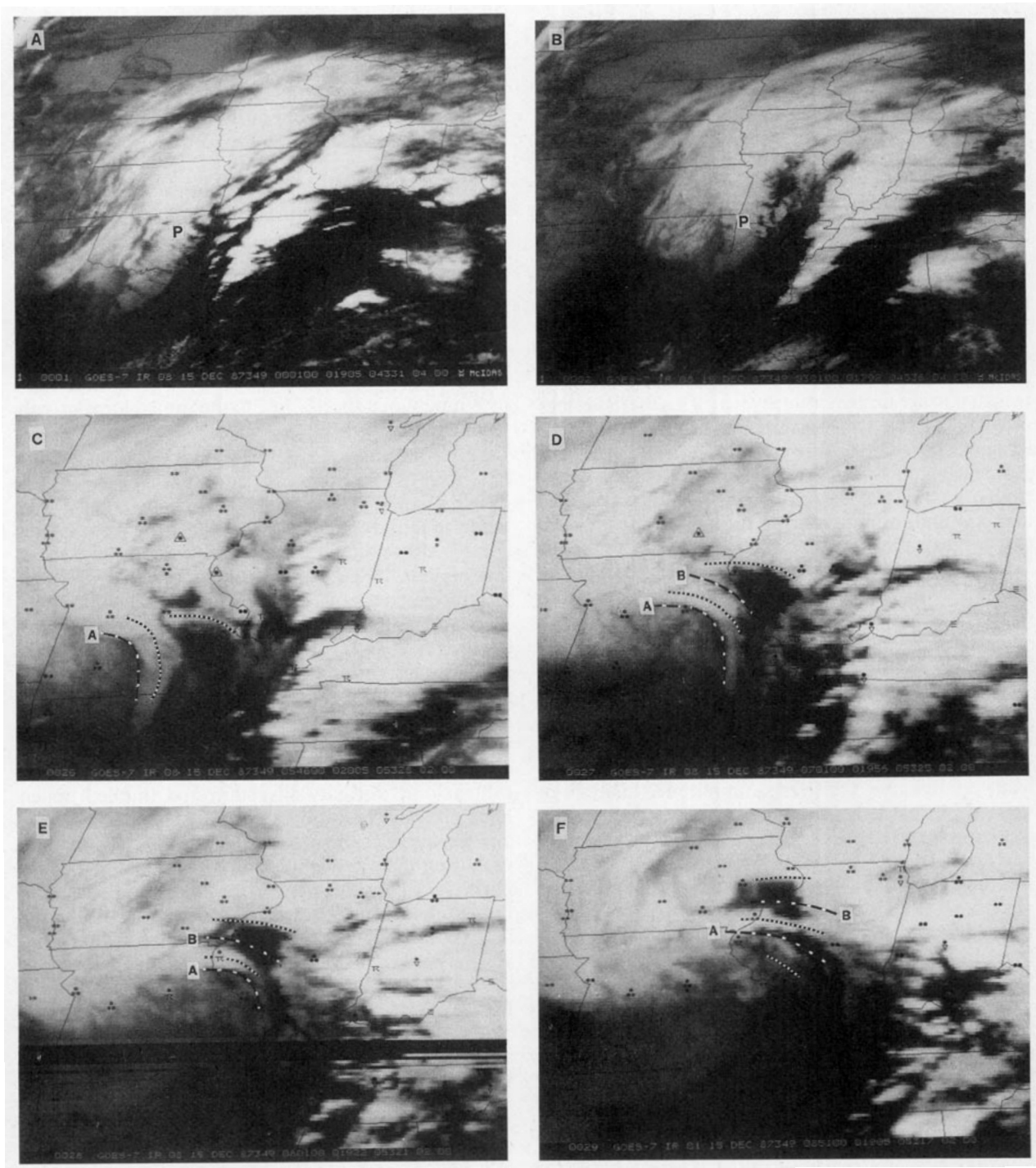

FIG. 8. Infrared satellite imagery from 15 December 1987 at (A) 0001 UTC, (B) 0301 UTC, (C) 0546 UTC, (D) 0701 UTC, (E) 0801 UTC, (F) 0851 UTC, (G) 1001 UTC, (H) 1046 UTC, (I) 1146 UTC, and (J) 1448 UTC. Locations of mesoscale wave-troughs (dashed lines), mesoscale pressure ridges (dotted lines), and surface weather symbols are also plotted on some images.

(Figs. 7b, 8c,d) and progressively increased from 255 K at 0400 UTC to 266 K at 0700 UTC as wave-trough A intensified.

Between 0600 UTC and 0700 UTC, wave-trough A passed both Vichy, Missouri (VIH) and Columbia, Missouri (COU) coincident with passage of the leading edge of the warm band which trails the small-scale comma cloud (Figs. 5, 6). But at 0730 UTC, a distinct pressure minimum was reported in the SA observations at Quincy, Illinois (UIN) (Fig. 10) that is inconsistent with the temporal evolution of wave-trough A isochrones and collocated with the leading edge of the

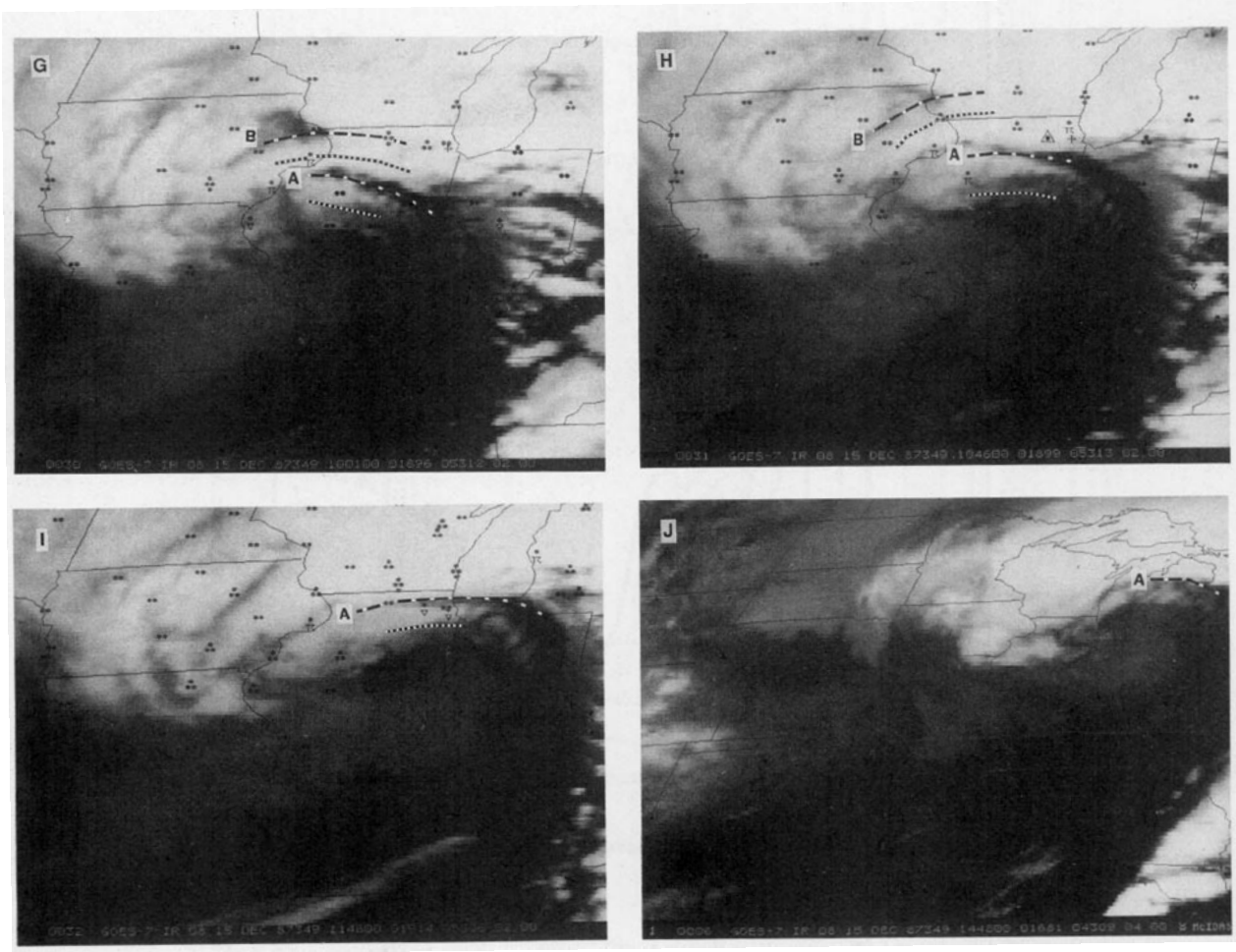

FIG. 8. (*Continued*)

small-scale comma cloud. This inconsistency was reconciled by postulating the existence of a second mesoscale pressure minimum (wave-trough B) along the leading edge of the comma cloud. The existence of wave-trough B allowed for continuity of wave-trough A to be maintained along the leading edge of the warm band (Figs. 7a,c; 8c,d,e). Passage of the outer edges of wave-trough A at UIN was largely undetected by temporally sparse SA observations, but was accompanied by a 2-mb pressure fall in 8 min at St. Louis, Missouri (STL). Consistent with these observations, the highest temperatures within the warm band associated with wave-trough A passed midway between UIN and STL as it moved northeastward across the Missouri–Illinois border. Therefore a peak-to-peak amplitude above 4 mb was retained in the analysis for wave-trough A within this data sparse region (Fig. 7b).

Consistency between satellite signatures of the mesoscale trough/ridge features and surface observations was largely retained as the waves propagated north-northeastward through Illinois between 0800 UTC and 1200 UTC (Figs. 8e,f,g,h,i). Despite greater coverage of surface data over the upper Midwest, satellite data was still used to help determine the orientation of wave trough and ridge axes. At 0900 UTC, a pressure ridge remained collocated with the cold (bright) cloud band that now extended eastward from near the intersection of the Illinois, Iowa, and Missouri borders (Figs. 8f, 9b). Mesoscale wave troughs A and B were located within warm IR blackbody temperatures just north and south of this cloud band. During the next 3 h, wave-trough B propagated northward along the Iowa–Illinois border before it dissipated in northeast Iowa and southwest Wisconsin (Figs. 7c,d) while wave-trough A intensified rapidly as it moved north-northeastward to the Illinois–Wisconsin border (Figs. 7a,b, 9c).

Detection of the mesoscale wave activity using infrared satellite imagery after 1200 UTC was complicated by propagation of the waves beneath the head of the large-scale comma cloud (compare Figs. 7a, 8i, j). Where the wave-disturbance signatures were obscured, the orientation of the wave-troughs were determined by requiring consistency between surface observations and wave-disturbance orientation based on extrapolation of cloud signatures in rapid-scan imagery. Between 1200 UTC and 1500 UTC, wave-trough A and the large-scale cloud shield deformed dramatically as they moved northeastward across the Great Lakes.

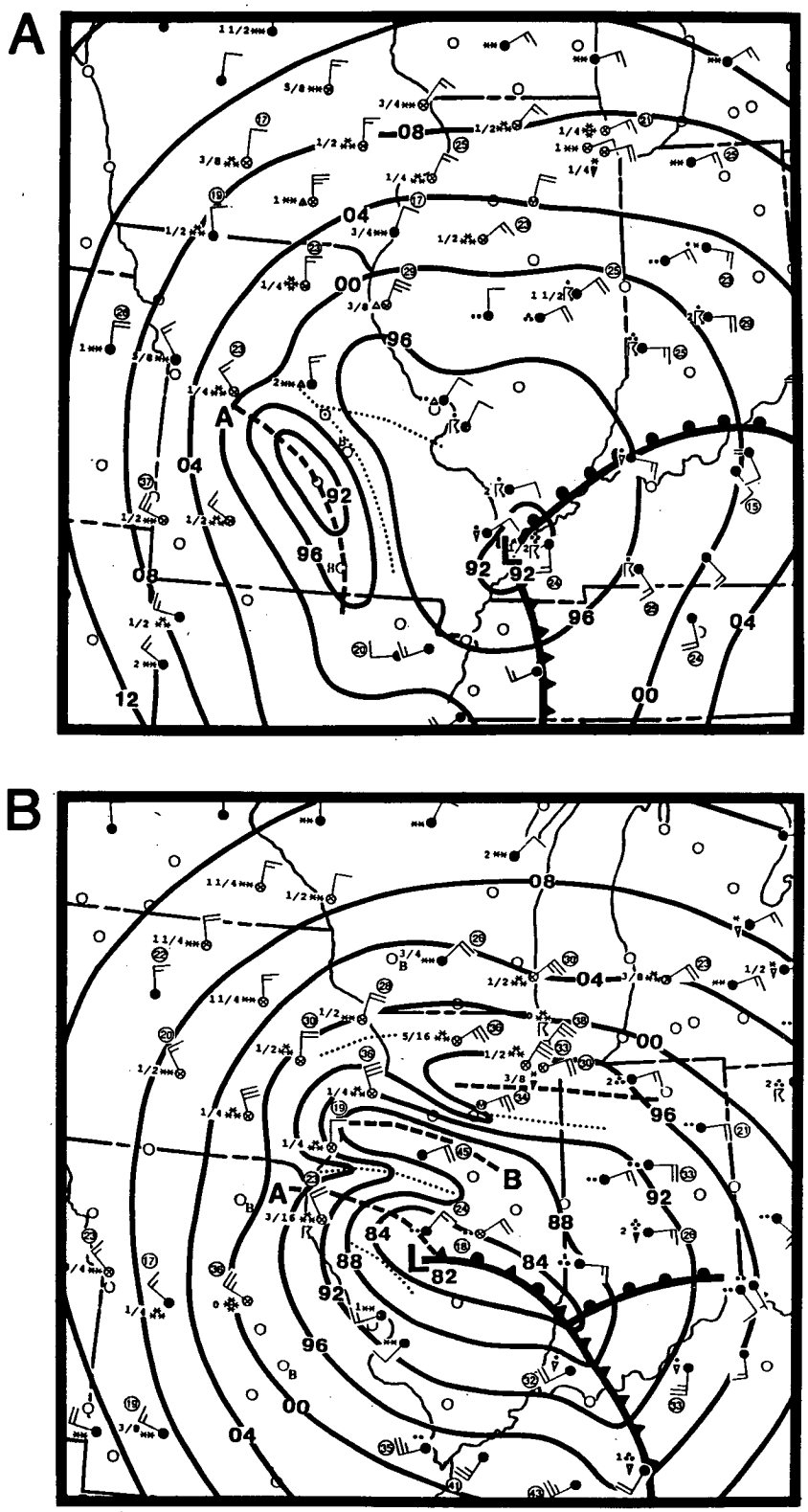

FIG. 9. Surface analyses of pressure (contoured every 4 mb) for (A) 0550 UTC, (B) 0850 UTC, (C) 1150 UTC, and (D) 1450 UTC with sustained winds (flags, kt), wind gusts (circled, kt), current weather, and visibility (<2 mi; mi) plotted for each station. Also plotted are the locations of mesoscale pressure troughs (dashed lines), mesoscale pressure ridges (dotted lines), cyclone circulation centers (L), and fronts.

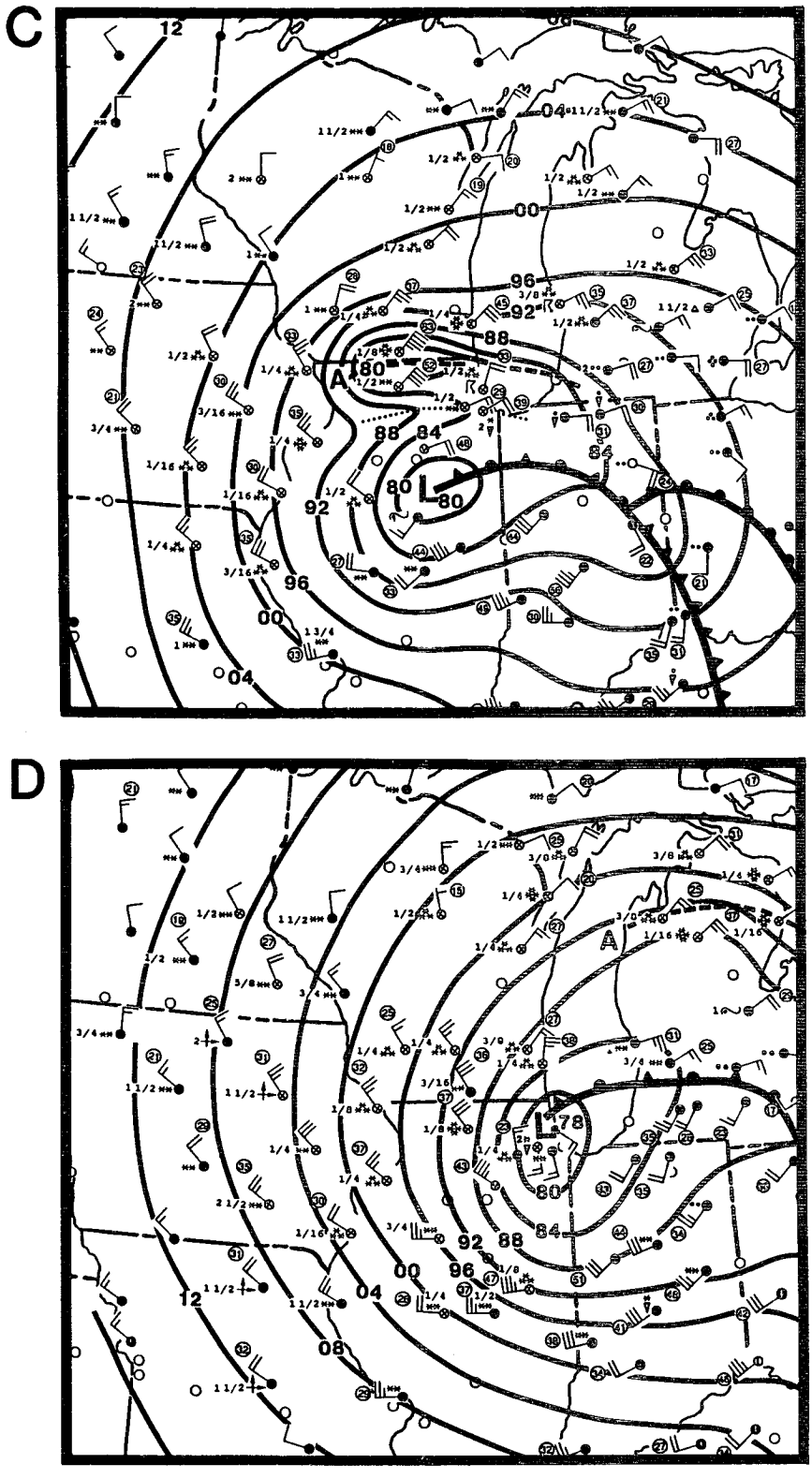

FIG. 9. (*Continued*)

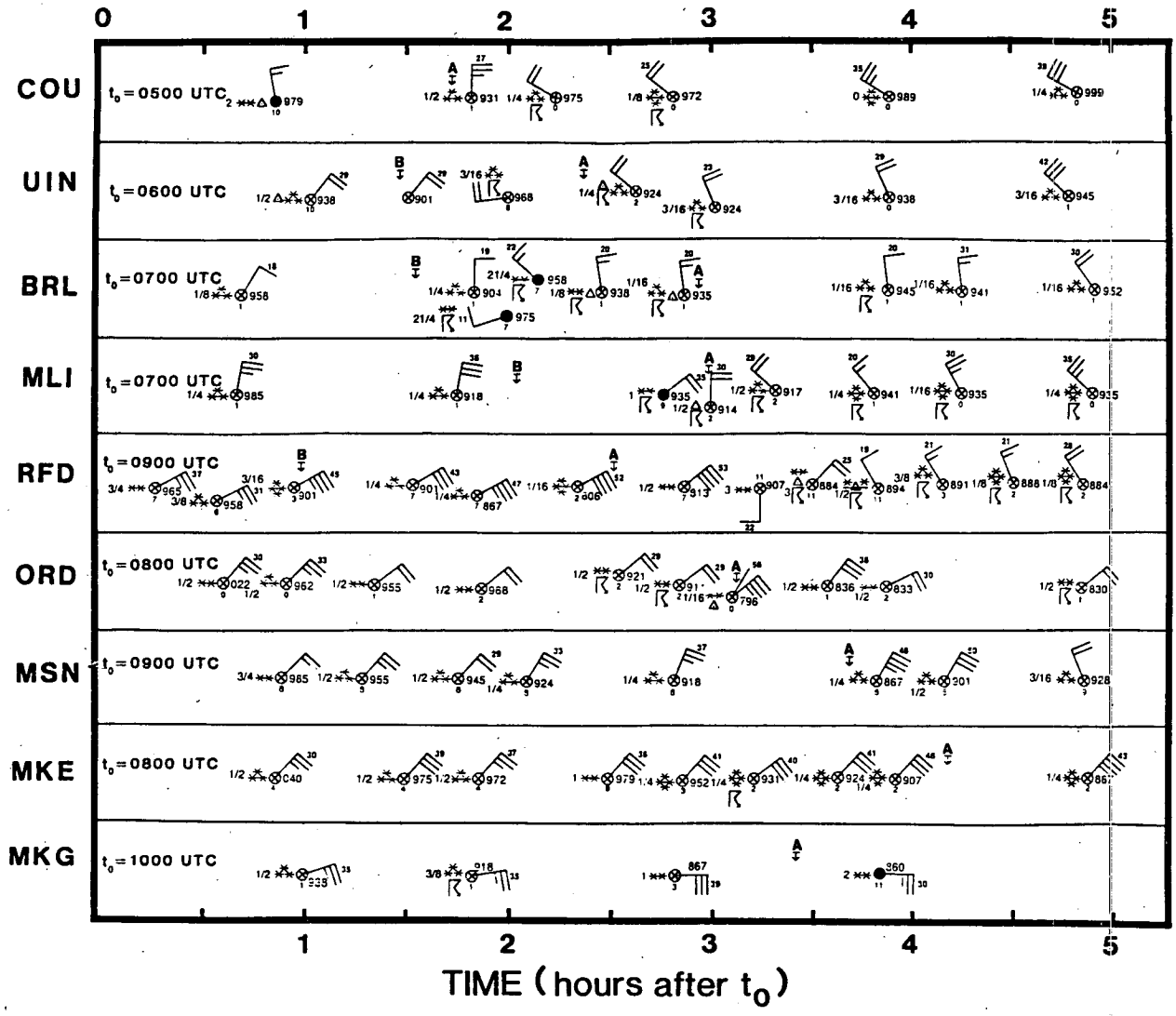

FIG. 10. Time series of surface observations over a 5-h period surrounding wave disturbance passage. The initial time (t_0, UTC) for each time series is plotted next to the three-letter station identifier (Fig. 5). Station plot includes sky cover, wind (1 barb = 10 kt (~5 m s^{-1})), wind gusts (at end of wind vector; kt), ceiling (below station; 100 feet), current weather, visibility (mi), and sea-level pressure (right of station; mb; leading '9' or '10' is omitted). Time of wave trough passage (A or B) is also noted for each station.

Similar curved wave-fronts were detected by Koch et al. (1988) using high resolution barograph data and satellite imagery.

4. Wave effects on surface weather

Interaction of the wave disturbances with the developing cyclone must be considered to understand the weather conditions observed over the Midwest between 0500 UTC and 1500 UTC 15 December 1987. This section documents wave disturbance interaction with the parent extratropical cyclone, and wave induced fluctuations in surface weather conditions.

a. Cyclone-wave interaction

Close interaction of wave-trough A with the extratropical cyclone center occurred southwest of Springfield, Illinois (SPI) between 0800 UTC and 1000 UTC during the rapid development stage of the cyclone (Fig. 9b). Because the surface pressure distribution was influenced by both the wave disturbances and developing cyclone, the position of the cyclone center during interaction with the wave disturbances was estimated subjectively from horizontal and temporal distributions of the wind field. Observations from SPI and Peoria, Illinois (PIA) (Figs. 11, 12) coincide with the passage of wave-trough A near the cyclone center. The coincidence of strong east-northeast winds with the distinct pressure minimum at each station was consistent with passage of an atmospheric gravity wave (wave-trough A) not with the center of an extratropical cyclone. In hourly surface analyses (Fig. 9b; 0800 UTC and 1000 UTC not shown) the cyclone center passed west of SPI

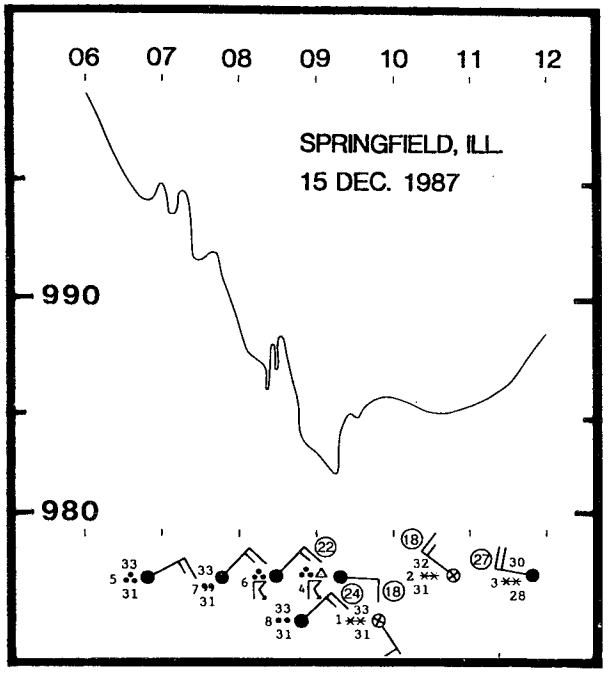

FIG. 11. Time series (UTC) of surface pressure and key surface observations (wind, kt; visibility, mi; temperature and dewpoint, °F) at Springfield, Illinois (SPI) on 15 December 1987.

(~0940 UTC) and southeast of PIA (~1100 UTC) (Fig. 7a) while wave-trough A moved north-northeastward at 30 m s^{-1}. As wave-trough A propagated

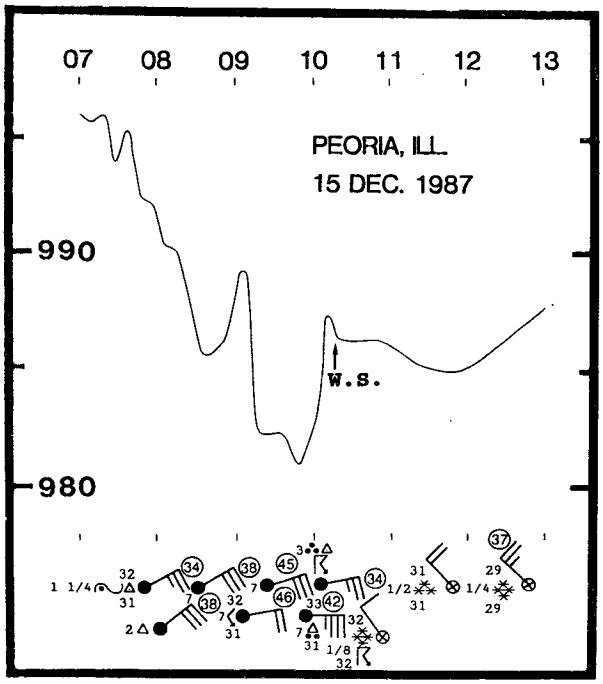

FIG. 12. Time series (UTC) of surface pressure and key surface observations (wind, kt; visibility, mi; temperature and dewpoint, °F) at Peoria, Illinois (PIA) on 15 December 1987. The time of a significant wind shift (WS) is indicated.

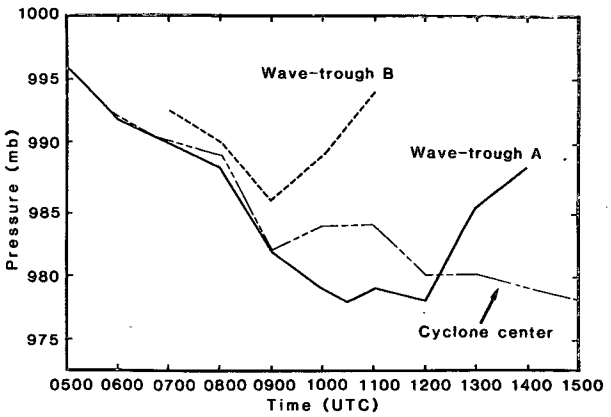

FIG. 13. Graph of minimum altimeter setting (mb) associated with the cyclone center (solid-dashed line), wave-trough A (solid line), and wave-trough B (dashed line) vs. time (UTC) on 15 December 1987.

through the cyclone center, the cyclone moved rapidly northward and its central pressure decreased 7 mb between 0800 and 0900 UTC (Fig. 13). After wave-trough passage (approximately 0900 UTC), the cyclone central pressure increased 2 mb in 1 h. Observations after 1100 UTC confirmed that the cyclone center moved slowly northeastward through eastern Illinois between 0900 UTC and 1500 UTC (Figs. 9c,d).

b. Evolution of surface winds and weather

Just as interpretation of surface cyclone evolution required consideration of the wave disturbances, understanding the weather which accompanied wave passage required consideration of the cyclone. The combined pressure gradient force and vertical motion produced by interaction of the wave disturbances with the developing cyclone could roughly be described by superposition of a simple, linear gravity wave (Fig. 3) on appropriate mean synoptic conditions. To the left of the cyclone track, the synoptic-scale geostrophic wind backed with time from northeast to northwest; ahead of the cyclone, the synoptic-scale geostrophic wind direction was consistently from the east. In both regions, the synoptic-scale geostrophic winds strengthened during the period of rapid cyclogenesis.

To understand wave disturbance-induced fluctuations in precipitation intensity, the synoptic-scale vertical motion and precipitation field had to be considered. Throughout the period, a 200-km wide synoptic-scale band of heavy snow extended from Missouri northeastward across the Wisconsin–Illinois border into central Michigan (Figs. 9a,b,c,d). At most stations, fluctuations in precipitation intensity were observed with wave disturbance passage that were consistent with gravity wave theory. At stations within the heavy snow band, wave disturbance passage was frequently followed by several hours of heavy snow with thunder. Outside of this band, only brief but intense wave-induced precipitation bands were observed.

Between 0500 UTC and 0800 UTC, the synoptic-scale pressure gradient west of the cyclone center combined with the rapid mesoscale pressure rise behind wave-trough A to produce strong northwest winds after wave passage. At Columbia, Missouri (COU) strong north winds associated with air accelerating towards the surface pressure minimum accompanied passage of wave-trough A at 0640 UTC (Figs. 9a, 10). During the next 20 min the pressure rose 4 mb, the wind shifted to the northwest, and heavy snow with thunder began. Heavy snow continued for the next 3 h with northwest winds gusting to 35 kt and near-zero visibility.

As both wave-trough A and wave-trough B moved northward ahead of the cyclone between 0900 and 1500 UTC, the horizontal pressure gradient ahead of the disturbances was strengthened by constructive interference of mesoscale and synoptic-scale pressure gradients. This interference created intense pressure gradients ahead of each mesoscale pressure trough as they propagated northward through Illinois and southern Wisconsin (Figs. 9b,c). The resulting winds gusted to over 50 kt and combined with heavy snowfall to create blizzard conditions.

At 0850 UTC, heavy snow was falling in a 150-km

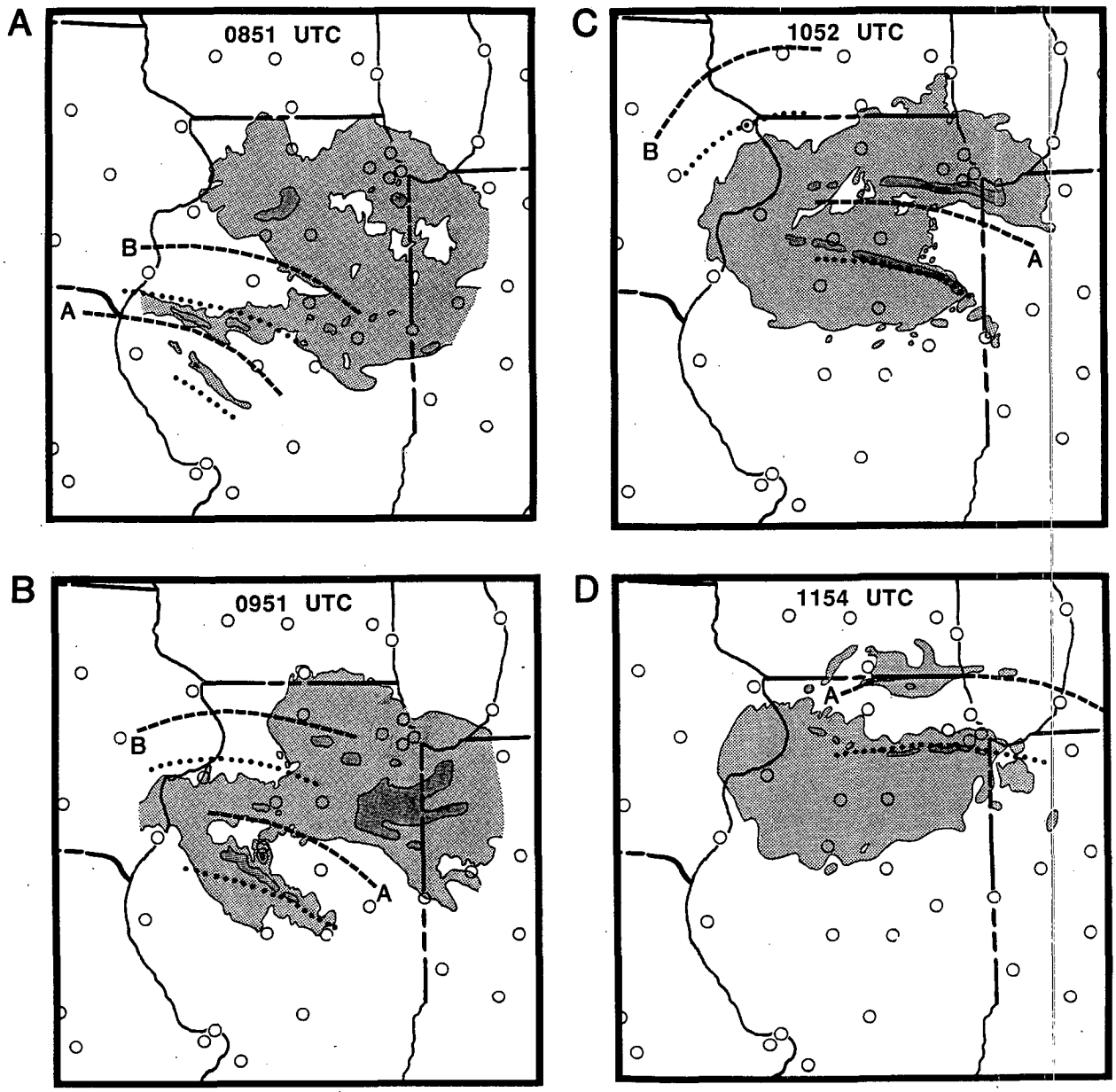

FIG. 14. Radar PPI scan on 15 December 1987 at (A) 0851 UTC, (B) 0951 UTC, (C) 1052 UTC, and (D) 1154 UTC from Marseilles, Illinois (MMO) with contours of intensity (VIP) level shaded in progressively darker tones for a 0.5° elevation angle and 125-n mi range. Station locations (open circles), mesoscale pressure troughs (dashed lines), and mesoscale pressure ridges (dotted lines) are also plotted.

wide arc extending from Columbia, Missouri (COU), northeastward to Moline, Illinois (MLI), and eastward to Grand Rapids, Michigan (GRR) (Fig. 9b). An intense pressure gradient ahead of wave-trough B helped produce sustained north winds of 28 kt at MLI where a pressure fall of 10 mb in 1 h was nearly complete. Near the trailing edge of wave-trough B at Burlington, Iowa (BRL), the surface pressure rose 7 mb in the next 10 min and the wind direction shifted from north to southwest as a mesoscale pressure ridge reached the station. Passage of this ridge was followed closely by heavy snow and ice pellets accompanied by thunder and lightning at both BRL and PIA (Figs. 10, 12). Within the synoptic-scale heavy snow band over BRL, thunder and heavy snow persisted for 2 h after surface pressure ridge passage. At PIA, which was east of the heavy snow band, a brief ice pellet thundershower lasted only 12 min.

Radar data from Marseilles, Illinois (MMO) captured the evolution of this and other intense precipitation bands that were closely linked to the wave disturbances (Fig. 14). At 0851 UTC, the line of strong convection (VIP level 2) trailed the mesoscale ridge axis (dotted line, Fig. 14a) which was about to pass BRL and PIA. Twenty min earlier, a maximum cloud top of 7.9 km was reported near the southeast end of the line. Wave-troughs A and B (dashed lines) were located in the echo-free regions (not precipitation free) ahead of and behind the convective line. Between 0851 UTC and 1052 UTC, the echo-free regions and heavy precipitation bands remained coupled with their respective mesoscale troughs and ridges as they propagated northeastward across northern Illinois (Figs. 14a,b,c). Maximum cloud top heights between 7.9 km and 8.9 km were reported with the southernmost convective line. When it passed PIA at between 1100 UTC and 1120 UTC, the line contained cloud-to-ground

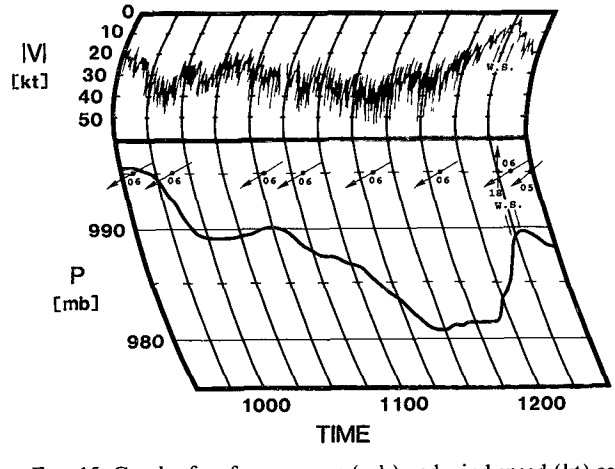

FIG. 15. Graph of surface pressure (mb) and wind speed (kt) as a function of time (UTC) for Rockford, Illinois (RFD) during passage of wave-trough B (0955 UTC) and wave-trough A (1125–1155 UTC) on 15 December 1987. The wind direction (arrows) and wind shifts (WS) are also indicated.

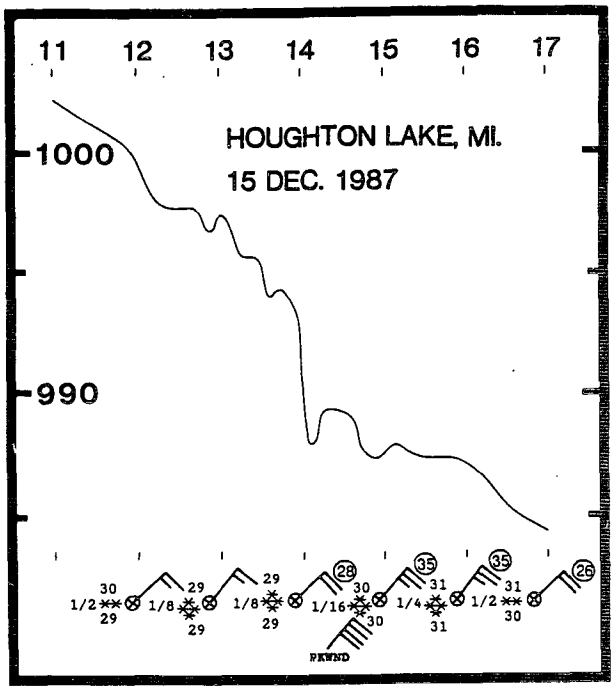

FIG. 16. Time series (UTC) of surface pressure and key surface observations (wind, kt; visibility, mi; temperature and dewpoint, °F) at Houghton Lake, Michigan (HTL) on 15 December 1987.

lightning and ⅛ mile visibility due to ice pellets and ⅛ inch hail (Fig. 12).

By 1050 UTC, wave-trough B was rapidly weakening as it moved northward into southwest Wisconsin and northeast Iowa (Figs. 7c,d), whereas the surface pressure gradient ahead of wave-trough A intensified as it propagated northward toward Chicago, Illinois through a strong synoptic-scale pressure gradient. Radar indicated an east–west line of strong convection (VIP level 3) ahead of pressure trough A (Fig. 14c). In the 16 min between 1050 UTC and 1106 UTC, the pressure at O'Hare Airport (ORD) in Chicago, Illinois fell 12 mb (Fig. 4a). A time-space transformation of this observation, assuming northeastward motion of wave-trough A at 30 m s^{-1}, *suggests a surface horizontal pressure gradient of 12 mb in 28 km* (15 mi)! As the pressure fell rapidly at O'Hare, the wind gusted to 56 kt and a heavy snow pellet shower reduced the visibility to 1/16 mi.

The surface analysis at 1150 UTC 15 December depicts the extraordinary pressure gradients and weather conditions associated with wave-trough A (Fig. 9c). Janesville, Wisconsin (JVL), located near the Wisconsin–Illinois border, reported the Midwest's lowest pressure (979 mb) with northeast winds sustained at 45 kt, gusting to 63 kt, and heavy snow which reduced the visibility to ⅛ mi. Rockford, Illinois (RFD), 40 km south of JVL, reported a pressure of 981 mb and sustained northeast winds at 39 kt with gusts to 53 kt. In the next 22 min the strong pressure gradient south of wave-trough A propagated past RFD and accelerated

air parcels moving southwestward toward the north. A pressure rise of 8.4 mb in 22 min at Rockford was accompanied by a rapid decrease in wind speed with a shift to weak south winds during the local pressure maximum at 1213 UTC (Fig. 15). The relative calm was broken by a brief return to northeast winds, the onset of thunder and lightning, and showers composed of snow and ice pellets. At 1237 UTC, the wind shifted to the northwest and a 3 h period of heavy snow with thunder began.

Marseilles radar from 1154 UTC (Fig. 14d) indicated strong convective precipitation collocated with the mesoscale pressure ridge south of wave-trough A. The intense echoes southwest of RFD were located in the strong pressure gradient associated with a shift from intense northeast winds to strong northwest winds (compare Figs. 9c, 14d). Over the next hour these echoes remained collocated with this wind shift, moved northeastward at 30 kt (against the flow up through the 700-mb level), and were associated with intense thunder ice pellet showers at RFD and JVL.

Between 1150 UTC and 1450 UTC, wave-trough A deformed dramatically as it propagated north-northeastward into northern Michigan (Figs. 7, 9c,d). Blizzard conditions were experienced at Madison (MSN), Milwaukee (MKE), and Muskegon (MKG), and Houghton Lake (HTL) (Figs. 10, 16) with wave-trough A passage. Heavy snow associated with the cyclone continued across western Illinois, most of Wisconsin, and northern Michigan (Fig. 9d). Strong northwest winds to the west of the cyclone caused drifting of the newly fallen snow. The occluded extratropical cyclone deepened 2 mb to 978 mb during the 3-h period, moved slowly northeastward through the Chicago area, and established a record for the lowest pressure observed at O'Hare Airport in December. By 1450 UTC wave-trough A was exiting northern Michigan and the cyclone had reached its lowest sea-level pressure (Figs. 7, 13). The sea-level pressure gradient became more uniform about the cyclone center (compare Figs. 9c,d) and the cessation of cyclone intensification was accompanied by the cessation of large-amplitude mesoscale wave-disturbance activity over the Midwest.

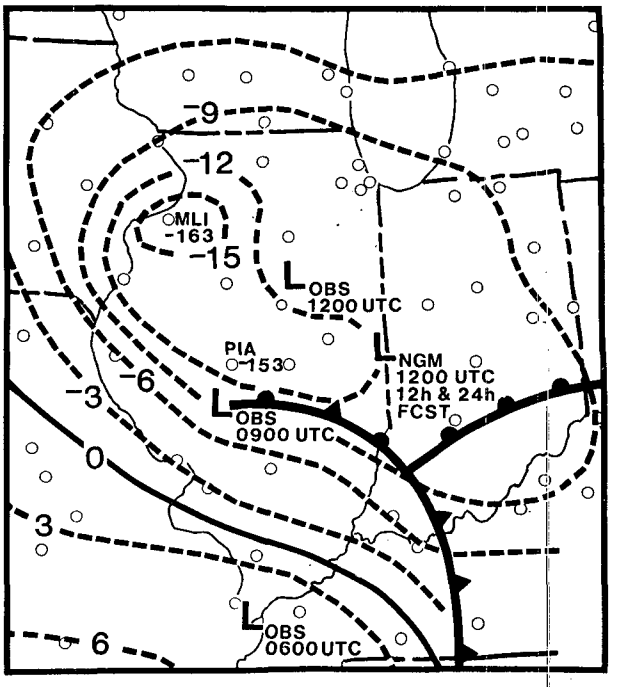

FIG. 17. Three-hour surface pressure change (dashed, mb) between 0550 UTC and 0850 UTC with positions of observed (0600, 0900, 1200 UTC) and NGM 12- and 24-h forecast (valid 1200 UTC) cyclone centers for 15 December 1987. The observed pressure change at two local minima (MLI and PIA; tenths of a mb) are also plotted.

5. Impact on operational weather forecasts and nowcasts

The large-amplitude mesoscale wave disturbances complicated the short-term forecasts for the 15 December 1987 cyclone. It was difficult, if not impossible, to separate the effects of mesoscale wave disturbances from those associated with the rapidly intensifying extratropical cyclone during the early morning hours of 15 December. Furthermore, a lack of awareness of the existence of these waves led to misinterpretation of the surface cyclone location which made even a nowcast of this storm a major challenge for forecasters.

The path of the observed or forecast surface cyclone is frequently used in collaboration with climatological data adjusted for the characteristics of the particular storm to corroborate or update model forecasts of heavy snow. Synoptic climatological studies find that the heaviest snow typically falls in a band 200–300 km to the left of the observed cyclone track (Fawcett and Saylor 1965; Goree and Younkin 1966; Harms 1973). In addition, forecasters occasionally exploit the tendency of cyclones to move toward the strongest surface pressure falls to make a short term forecast of the cyclone track independent of the most recent numerical guidance (Petterssen 1956). If this forecast technique is employed, proper interpretation of both the station pressure and pressure tendency is essential.

Consider the conditions in the Midwest at 0850 UTC 15 December (Fig. 9b). Moderate and heavy snow was reported approximately 75–250 km (50–150 mi) to the northwest and north of the cyclone center. The largest 3-h surface pressure falls were north and northwest of the cyclone center at Peoria (PIA) and Moline, Illinois (MLI) (Fig. 17). If the cyclone was forecast to move from its 0850 UTC position toward the location of strongest pressure falls, the forecast position would be 120 km west of the observed location and 200 km west of National Meteorological Center Nested Grid Model (NGM) forecasts. Earlier NGM forecasts had predicted the cyclone would move through western Illinois into central Wisconsin, with heavy snowfall extending into central Iowa and southeast Minnesota, and with a commensurate westward shift of the boundary between rain and snow. If guidance from the observed pressure falls were followed, the forecast axis

of heavy snowfall would be erroneously shifted to the west in agreement with the earlier model forecasts.

Determination of the actual cyclone track was made difficult between 0850 UTC and 1250 UTC because the minimum analyzed surface pressure associated with wave-trough A was lower than the pressure at the cyclone center (Figs. 9d, 13). The barograph trace and wind observations from O'Hare Airport highlight the differences between passage of wave-trough A at 1106 UTC and passage of the cyclone center at 1430 UTC (Fig. 4a). The distinguishing characteristic of the pressure minimum associated with wave-trough A is that it was accompanied by a maximum in the wind velocity in accord with linear gravity wave theory. Passage of the cyclone center was accompanied by a broad minimum in surface pressure and relatively weak surface winds.

The rapid northward movement of wave-trough A viewed with the coarse temporal resolution of the SA observations increased the confusion. Between 0850 UTC and 1150 UTC, the succession of Midwest minimum altimeter setting observations at Peoria, Marseilles, Rockford, and Janesville suggested that the cyclone center had moved rapidly northward from central Illinois into southcentral Wisconsin. Although timely warnings were issued by the Madison, Wisconsin Weather Service Office for abrupt changes in weather conditions associated with wave-trough A, a special weather statement issued at 1420 UTC suggested that passage of wave-trough A was mistaken for passage of the cyclone center. The final paragraph read . . .

> "The wind at Truax Field (MSN) dropped to near calm about 710 AM (1310 UTC) this morning as the center of the storm passed nearby. It was like being in the eye of a hurricane. The winds did pick up once the center passed northeast of Madison."

At this time, the actual surface cyclone center was approximately 100 km south of Chicago.

Forecasters have had mixed results in dealing with other large-amplitude mesoscale wave disturbances. For the 27–28 February 1984 gravity wave case documented by Bosart and Seimon (1988), strong pressure falls were correctly interpreted as a gravity wave by one forecast office but incorrectly interpreted by other operational meteorologists as the onset of secondary cyclogenesis along a coastal front. These types of misinterpretations undoubtedly influence short-term forecasts in critical weather situations and point to the need for forecasters to recognize weather conditions associated with large-amplitude mesoscale wave disturbances.

A second major operational problem posed by the large-amplitude wave disturbances was their rapid modification of even well-forecast synoptic-scale weather conditions into highly dangerous, locally severe conditions (discussed in section 4). Between 0750 UTC and 1455 UTC on 15 December 1987, the combination of high winds (Fig. 18), heavy snow, and cloud-to-ground lightning created blizzard conditions hazardous to humans and livestock, caused power outages, forced the closure of many roads and airports, and damaged property in northern Illinois, eastern Iowa, and southern Wisconsin (Storm Data 1987).

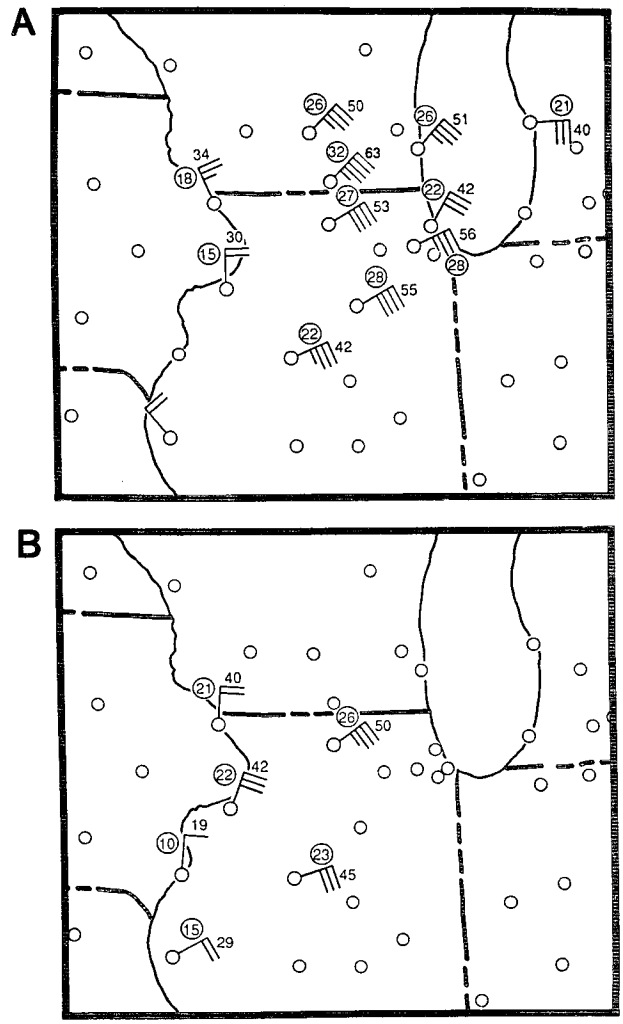

FIG. 18. Observations of the maximum sustained wind (full barb = 10 kt (~5 m s^{-1})) and gusts [kt (bold) and m s^{-1} (circled)] during passage of (A) wave-trough A, and (B) wave-trough B. The observations span the time period between 0700 UTC and 1300 UTC 15 December.

Severe blizzard conditions accompanied mesoscale wave-trough A as it moved northward through northern Illinois and southern Wisconsin. At 1117 UTC, only 11 min after passage of wave-trough A, O'Hare International Airport closed for only the fourth time in the last 20 years. Blizzard warnings were issued for extreme southeast Wisconsin at 1220 UTC after wave-trough A crossed the Illinois–Wisconsin border (Fig. 9c). With up to 15 cm of new snow already on the ground, heavy snow accompanied by winds which gusted to at least 63 kt created near-zero visibilities that forced road closures and suspension of plowing operations across portions of the warning area. At 1310

UTC, just after wave-trough A passed Truax Field (MSN), the blizzard warning was extended westward to include Madison, Wisconsin. Even after wave-trough A moved out of Wisconsin, marginal blizzard conditions continued until 1700 UTC across Illinois and southern Wisconsin within the strong northwest winds west of the cyclone center (e.g., MSN, RFD in Figs. 9d, 10).

A dangerous characteristic of wave-disturbance A was the near calm conditions and cessation of precipitation which accompanied the rapid pressure rise after wave-trough passage (e.g., RFD; Fig. 4b). Despite special weather statements which warned of an imminent deterioration in weather conditions, the public could easily have misinterpreted the calm conditions and assumed the storm was over. The relative calm was followed by a snow and ice pellet shower accompanied by lightning, a shift to strong northwest winds, and up to three more hours of heavy snow. Cloud-to-ground lightning started several damaging fires in southern Wisconsin (Storm Data 1987) and has also been observed with a large-amplitude mesoscale wave disturbance embedded in an intense East Coast blizzard (Bosart and Sanders 1986).

6. Application of theory to understand and forecast mesoscale wave disturbances

a. *Background*

Atmospheric gravity wave theories provide valuable insights into the structure and dynamics important in mesoscale wave disturbance formation and maintenance. Hooke (1986), Uccellini and Koch (1987), and Koch and Dorian (1988) include overviews of theoretical and diagnostic investigations of atmospheric gravity waves. Atmospheric gravity waves generated by flow over mountains are not discussed in this article but are summarized by Durran (1986). Other diagnostic studies of long-lived, large-amplitude waves similar to 15 December 1987 include Bosart and Cussen (1973), Uccellini (1975), Pecnick and Young (1984), Bosart and Sanders (1986), and Bosart and Seimons (1988). This section discusses atmospheric structure and processes important to long-lived, large-amplitude gravity wave maintenance and formation, with emphasis on the practical application of these concepts to the mesoscale wave disturbances of 15 December 1987.

b. *Wave disturbance characteristics*

The horizontal phase velocity of the wave disturbances must be estimated in order to: 1) estimate the horizontal wavelength of the waves, 2) estimate the effectiveness of ambient synoptic conditions in trapping wave energy, and 3) construct the time-space transformations used in this study. The phase velocity describes the motion of individual wave components (each small perturbation in surface pressure) which comprise the total wave disturbance. The group velocity of a wave disturbance describes the movement of zones of constructive interference between individual wave components. As such, the group velocity also describes the propagation velocity of wave energy as manifested by the maximum amplitude in pressure perturbation.

Some atmospheric waves (e.g., Rossby waves and short-wavelength gravity waves) are dispersive, which means that the propagation velocity of individual wave components is a function of their wavelength. Phase velocities differ from the group velocity for dispersive waves. Thus the structure of a dispersive gravity wave changes with time resulting in different barogram signatures as it passes each observation station. Near-constant characteristic barogram traces result from nondispersive or only slightly dispersive waves. Gravity waves of long wavelength, like those observed on 15 December 1987, are nearly hydrostatic and therefore have little horizontal dispersion. Nonlinear solitary waves and cnoidal waves (a family of solitary waves) (Christie et al. 1978; Christie 1989) are also nondispersive and may be a more suitable model for some large-amplitude disturbances (Pecnick and Young 1984). Fortunately, the atmospheric conditions favorable for maintenance of nonlinear solitary waves appear to be similar to those required for maintenance of the more extensively studied linear gravity waves (Skyllingstad 1986). These conditions will be described in the next section.

The barograms in Fig. 6 do not all look similar to each other. However, the structure of the barogram traces does remain nearly constant with time for different sections of the wave. A sharp pressure minimum, estimated as 6 km in width, and strong northeast winds were observed as the central and eastern segments of wave-trough A passed O'Hare Airport (ORD), Milwaukee, Wisconsin (MKE), Muskegon, Michigan (MKG), and Houghton Lake, Michigan (HTL) with only slight recovery after passage of the pressure minimum (Figs. 4, 6, 9, 10, 16). In contrast, a broad minimum in surface pressure, estimated at 40 km wide, was observed as the western section of wave-trough A passed Peoria (PIA), Marseilles (MMO), Rockford (RFD), and Madison (MSN). During the broad minimum at Rockford, two intervals of strong sustained northeast winds approximately 25 min apart were separated by a small pressure rise accompanying the relative minimum in wind speed (Fig. 15). Similar small

TABLE 1. Average phase velocity estimates.

Feature	Time period (UTC)	Average phase velocity
Wave Trough A	0500–1000	from 225° at 32 m s^{-1}
	1000–1400	from 218° at 34 m s^{-1}
Wave Trough B	0800–1000	from 190° at 31 m s^{-1}

The method of estimation is described in the text.

pressure rises were observed during the broad pressure minimum at PIA and MMO (Fig. 6).

The phase velocity was estimated assuming it was equal to the group velocity. Therefore it represents the propagation velocity of the large-amplitude wave disturbances. To estimate this velocity, the isochrones were connected at the centroid of maximum wave amplitude, yielding crude estimates of direction and speed (Table 1). Cross-spectral analysis (Stobie et al. 1983; Koch and Golus 1988) would produce far more detailed results, but requires denser data coverage than was available. Therefore it was not attempted.

For the 15 December wave disturbances, as in other similar studies (e.g., Koch and Golus 1988), estimation of the phase velocity was complicated by the large spacing of the surface barograph network and the significant curvature of the observed wave fronts (Figs. 5, 7). Substantial variations in phase velocity were apparent along individual wave fronts and between wave-trough A and wave-trough B. A phase velocity of 32 m s^{-1} from 225° will be used in subsequent discussions because it was appropriate for wave-trough A as it passed the Monett, Missouri (UMN) radiosonde station.

The wavelength is determined by multiplying the observed wave period by the estimated phase speed and is corroborated by measuring the separation between trough and ridge axes estimated in IR satellite, radar, and synoptic data. Estimates of the wave periods range between 50 and 90 min with horizontal wavelengths between 90 and 180 km. The longer wavelengths and periods are for the broad pressure minima observed in Missouri, wave-trough B, and western sections of wave-trough A over Illinois. If the broad pressure minima with wave-trough A between 1000 UTC and 1300 UTC was composed of two wave components as suggested by observations at Rockford (Fig. 15), most stations indicate horizontal wavelengths near 100 km for wave-trough A between 1000 UTC and 1500 UTC. All these values are similar to the wave characteristics found by Uccellini and Koch (1987) in their review of documented mesoscale wave disturbances.

A time-space transformation of the surface wind data during the rapid pressure rise at Rockford, Illinois between 1150 UTC and 1215 UTC indicates convergence of approximately 5×10^{-4} s^{-1}. This is comparable to the magnitude of convergence in several other documented gravity waves (Pecnick and Young 1984; Bosart and Seimon 1988) and with an observed cold front (Sanders 1955), but nearly ten times larger than that expected in an intense synoptic-scale system (Petterssen 1956).

c. *Vertical structures conducive to wave maintenance*

The vertical profile of temperature and wind in the wave environment are crucial to wave propagation, maintenance, and formation (see Hooke 1986). Under typical atmospheric conditions, gravity wave energy is free to propagate vertically, which in the absence of a continuous generation mechanism results in the loss of coherent wave structure within about one horizontal wavelength (Uccellini and Koch 1987). Lindzen and Tung (1976) detailed specific atmospheric conditions, called a wave duct, which reduces vertical propagation of wave energy and can result in long-lived gravity waves. Although other atmospheric conditions can also substantially reduce vertical propagation of wave energy (Chimonas and Hines 1986; Koch and Dorian, 1988), conditions over the Midwest on 15 December 1987 conform closely to Lindzen and Tung's (1976) wave duct theory which consists of four criteria.

The first criterion for an effective gravity wave duct is the presence of a layer of strong static stability. Horizontal propagation of the wave disturbance is associated with vertical displacements of this statically stable layer. The 0000 UTC 15 December rawinsonde observation from Monett, Missouri (UMN), the best available measurement of atmospheric conditions during the initiation of mesoscale wave disturbances A and B, indicates a near-isothermal layer between 890 mb and 670 mb (2.3 km thick) (Fig. 19). Analysis of 0000 UTC rawinsonde observations at Salem, Illinois (SLO) and Peoria, Illinois (PIA) reveals similar low-level isothermal layers 3.0 km and 2.7 km thick, respectively.

The second criterion is that the stable layer is sufficiently thick. The depth of this stable layer determines the phase velocities that the wave duct is able to support. The phase velocity of the dominant wave component should be

$$C_{\text{duct}} = \frac{2}{\pi}\left[\frac{gD(\theta_T - \theta_B)}{\bar{\theta}}\right]^{1/2}, \qquad (1)$$

where g is the acceleration due to gravity, D is the thickness of the wave duct, and θ is the potential temperature at the top (T), bottom (B), and average (-) within the stable layer. As a result, consistency with Lindzen and Tung's wave duct theory requires that the observed stable layer must be thick enough to contain one-quarter of the vertical wavelength corresponding to the observed phase speed or

$$D > \frac{\pi}{2}\frac{(C - U_*)}{N}, \qquad (2)$$

where C is the observed phase speed of the wave, U_* is the observed wind in the direction of wave propagation, and N is the Brunt-Väisälä frequency (U_* and N are mean values for the stable layer). From the Monett, Missouri rawinsonde observation, $U_* = 8$ m s^{-1}, $N = 0.02$ s^{-1}, and recall $C \simeq 32$ m s^{-1}. The computed minimum thickness, $D = 1.8$ km, is slightly exceeded by the observed stable layers at Monett, Missouri; Salem, Illinois; and Peoria, Illinois.

The third requirement for an effective wave duct is the presence of conditional instability (a reflecting layer) above the layer of high static stability. As the lapse rate of the layer approaches neutral stability, the layer traps energy within the stable layer more effec-

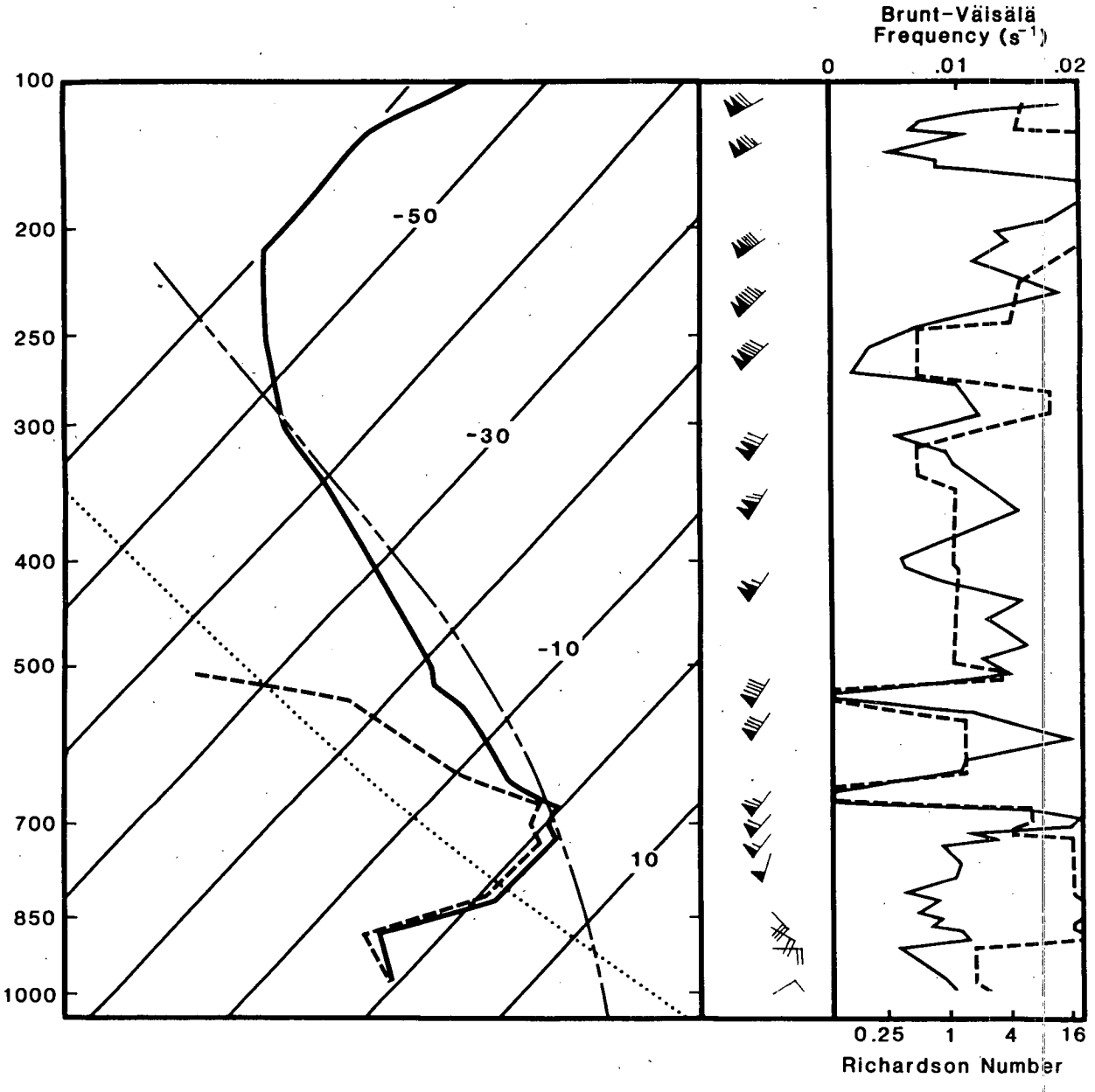

FIG. 19. Vertical profiles of temperature (solid, °C), dewpoint (dashed; °C), and wind velocity (long barb = 5 m s^{-1}) in Skew T –log P format for 0000 UTC 15 December 1987 at Monett, Missouri (UMN). Reference isotherms (thin solid), dry adiabat (dotted), and pseudo-adiabat (long-short dashed) are provided. Corresponding vertical profiles of Richardson number (thin solid; scale on the bottom) and Brunt-Väisälä frequency (dashed; s^{-1}; scale on the top) are plotted to the right of the sounding.

tively. At 0000 UTC 15 December, near-neutral lapse rates in near-saturated layers are found directly above the low-level stable layer at Monett (Fig. 19), Salem, and Peoria.

The areal extent and temporal evolution of the low-level stable layer (described by T(700 mb) − T(850 mb)), the layer of weak mid-level stability (T(500 mb) − T(700 mb)), and the region where they overlap is described in Fig. 20. The 700-mb level corresponded with the top of the stable layer over most of the Midwest. At 0000 UTC 15 December (Fig. 20a), a low-level isothermal layer (light shading) was located north and west of the 850-mb warm front. The mid-level layer of moist neutrality only overlapped the southern half of this region but effectively delineated the region of large-amplitude wave disturbance genesis. Because the stable layer at Peoria extends above 700 mb, the moist neutrality that was present from 670 to 500 mb is not depicted in this figure. By 1200 UTC, the region of overlap was swept northeastward ahead of the extratropical cyclone to a location collocated with wave-trough A (Fig. 20b). The analysis in the vicinity of

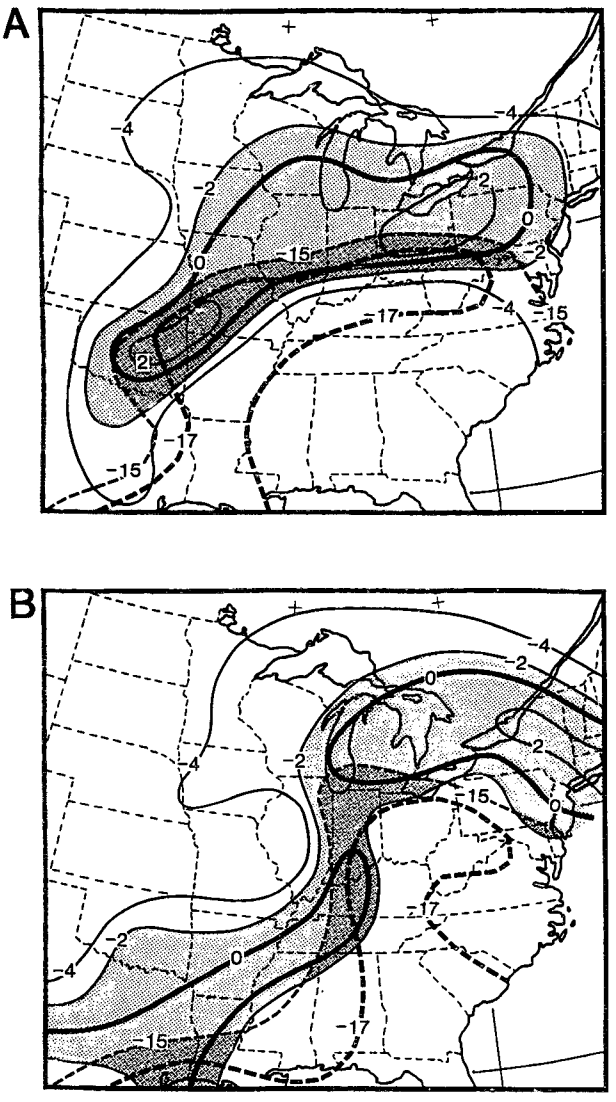

FIG. 20. Low-level (T (700 mb) − T (850 mb); solid, °C) and mid-level (T (500 mb) − T (700 mb); dashed, °C) static stability analysis for (A) 0000 UTC and (B) 1200 UTC 15 December 1987. Light shading highlights the region of strong low-level static stability; dark shading indicates where weak mid-level stability overlaps the low-level stable layer. The top of the low-level stable layer over the Midwest is found at approximately 700 mb (e.g., UMN). The temperature change between 700 mb and 500 mb following the moist adiabatic lapse rate for a parcel initially at 0°C (850 mb) is −17°C.

this wave-trough is based on a conservative hand analysis of the 850-mb, 700-mb, and 500-mb thermal patterns. The intense baroclinic zones observed by aircraft in these systems (Shapiro and Kennedy 1981; Keyser and Shapiro 1986) were not included, and contribute to the uncertainty as to the exact nature of the wave environment.

The reflection of wave energy by the conditionally unstable layer can be increased by the existence or near-existence of a critical level (steering level). A critical level exists where the environmental wind speed in the direction of wave propagation (U_*) equals the wave's phase speed (C = 32 m s^{-1}). The reflection efficiency at the critical level is determined by the Richardson number (Ri), which measures the dynamic stability of the environmental wind shear and can be written

$$Ri = \frac{g}{\theta}\frac{\partial\theta}{\partial z}\left[\left(\frac{\partial u}{\partial z}\right)^2 + \left(\frac{\partial v}{\partial z}\right)^2\right]^{-1/2}. \quad (3)$$

It is called the bulk Richardson number when it is evaluated using finite differences of observed data (e.g., Stull 1988). If a critical level occurs within the conditionally unstable layer and is accompanied by a bulk Richardson number less than 1.0, wave energy will be effectively maintained or in some cases increased (Ferretti et al. 1988). The 0000 UTC 15 December rawinsonde observation at Monett, Missouri indicated a critical level (U_* = C = 32 m s^{-1}) at 640 mb, within a near-saturated reflecting layer and accompanied by a bulk Richardson number near zero (Fig. 19). Nearly identical critical level conditions were also observed downstream at Salem, Illinois (not shown). Observations indicate that the critical level instability can form within only a few hours of the wave event (Ferretti et al. 1988). This fact, coupled with difficulties in determining wave phase velocities, *make real-time detection of the presence and location of unstable critical levels difficult, if not impossible, using the current operational observing network.*

The fourth criterion is that a critical level does NOT exist within the low-level stable layer. A critical level with a large Richardson number absorbs wave energy and would cause the wave to rapidly dissipate.

All four Lindzen and Tung (1976) criteria must be met for a strong wave duct to support long-lived large-amplitude waves. The first two criteria allow for large-amplitude waves; the last two are important for maintenance of that amplitude for many hours. Despite uncertainties in the phase velocity estimates and the true vertical wind profile at the time the waves passed the radiosonde stations, observations over the Midwest from 15 December 1987 indicate the presence of a strong wave duct capable of maintaining the mesoscale wave disturbances for an extended period of time.

d. Atmospheric structures and processes important for wave formation or intensification

The presence of a dynamically unstable critical level (Ri < 0.25 or bulk Ri < 1.0) indicates the potential for gravity wave initiation, maintenance, or intensification through extraction of kinetic energy from the environmental wind shear of the unstable layer (Lindzen and Tung 1976; Stobie et al. 1983; Fritts 1984; Ferretti et al. 1988; Koch and Dorian 1988). Stobie et al. (1983) indicate that this energy source can be important to maintain wave energy against the dissipative effects of friction and vertical energy propagation. The presence of sufficiently small Richardson numbers over much of the Midwest during the large-amplitude wave activity on 15 December 1987 suggested that this pro-

cess was instrumental in maintenance and amplification of the observed waves. However, the existence of these conditions over a broad area contrasts with the localized nature of the largest waves and suggests that it was not the sole contributor to wave generation.

Latent heat release associated with moist convection is also capable of mesoscale wave disturbance generation or intensification. Several observational studies document wave generation or amplification through cooperative interaction between the wave and deep convection (summarized in Koch et al. 1988). The position of convection 1 h before wave detection in southwest Missouri is roughly summarized in the manually digitized radar from 0235 UTC (Fig. 21). The most intense convection was southeast of the genesis region. Comparison of satellite imagery with the radar summary (compare Figs. 8b, 21) combined with the association of wave-trough A with the trailing edge of the cloud band (*P*), suggested that wave trough A organized near the trailing edge of the precipitation shield in extreme northeast Oklahoma and southwest of the precipitation with cloud tops to 5.8 km. Microfilm copies of the Monett, Missouri radar were difficult to read, but did not seem to indicate strong convection accompanying wave passage.

Radar data from Marseilles, Illinois (Fig. 14) discussed in section 4 revealed that between 0851 UTC and 1154 UTC, the wave-troughs were adjacent to lines of strong convection, where convectively induced subsidence could have enhanced wave-induced warming of the low-level stable layer. Bosart and Seimon (1988) indicated that their large-amplitude wave formed and intensified slightly behind a line of strong thunderstorms over the southeast United States. Although cause and effect could not be determined with the present data set, cooperative interaction between convection and the wave disturbances was possible.

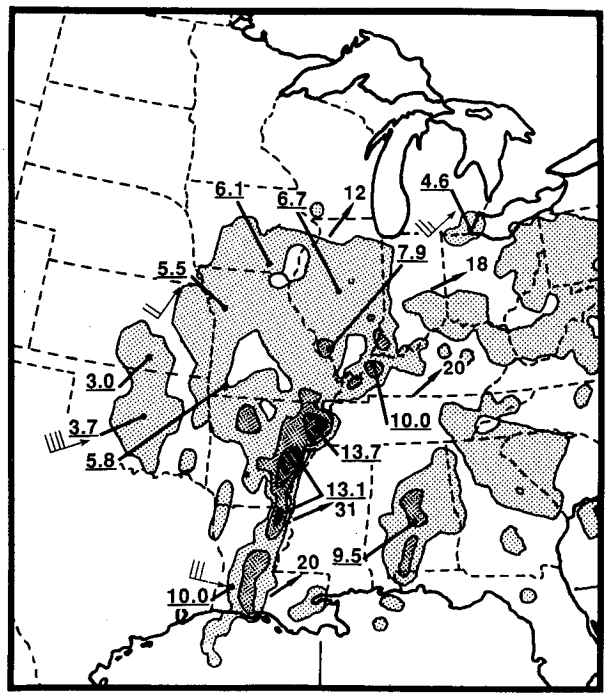

FIG. 21. NWS manually digitized radar intensity (VIP) map for 0235 UTC. Contours indicate VIP levels 1, 3, and 5 which are shaded progressively darker. Cloud top heights (km) are underlined, cell movement (m s^{-1}) is indicated by an arrow, and area movement (m s^{-1}) is indicated by wind barbs.

Generation of gravity waves during mass-momentum (geostrophic) adjustment has been documented theoretically (e.g., Rossby 1938; Cahn 1945; Matsumoto 1961). Review of the synoptic conditions associated with 13 different long-lived, large-amplitude mesoscale wave disturbances suggests that their initiation frequently results from mass-momentum adjustments near jet streaks (Uccellini and Koch 1987). The region of wave activity is generally bounded to the west and northwest by the axis of the polar jet stream, to the southeast by a surface front, to the northeast by an upper-level ridge axis, and to the southwest by the inflection point between the downstream, upper-level ridge axis and upstream trough axis. The association of the southern boundary of the wave activity with a surface front indicates the frequent coincidence of fronts with the southern boundary of the low-level stable layer. The approach of a strong jet streak to the upper-level ridge axis is also common to the wave disturbance episodes. As jet stream parcels approach the anticyclonic relative vorticity environment of the ridge axis, mass-momentum imbalances can result in the generation of inertia-gravity waves (Coriolis force important) which attempt to restore balance (Uccellini and Koch 1987).

The characteristics of the environment accompanying the 15 December wave disturbances correspond closely to those isolated by Uccellini and Koch (1987) (Fig. 22). The 320-K isentropic surface at 0000 UTC 15 December (Fig. 22a) slices through the polar jet as it slopes from 250 mb near the trough axis to 500 mb in the southeast United States. At 0000 UTC, the wave genesis region was under the axis of maximum winds which stretched northeastward from central Oklahoma into Iowa on the 320-K isentropic surface (Fig. 22a). The large-amplitude wave disturbances occurred northwest of the warm front and between the inflection axis in the stream function field (thick dashed lines) and the downstream ridge axis (thick dotted lines) over the upper Midwest. Between 0000 UTC and 1200 UTC, the large-amplitude wave activity shifted to the northwest of the jet stream axis as an intense jet streak accompanied by a highly curved upper-level trough propagated rapidly northeastward toward the quasi-stationary ridge axis (Fig. 22b).

Geostrophic adjustment during frontogenesis can also generate atmospheric gravity waves (Ley and Peltier 1978). The waves are generated from imbalances between the along-front wind and the cross-front temperature gradient caused by rapid deformation of the lower-level thermal structure. In this theoretical

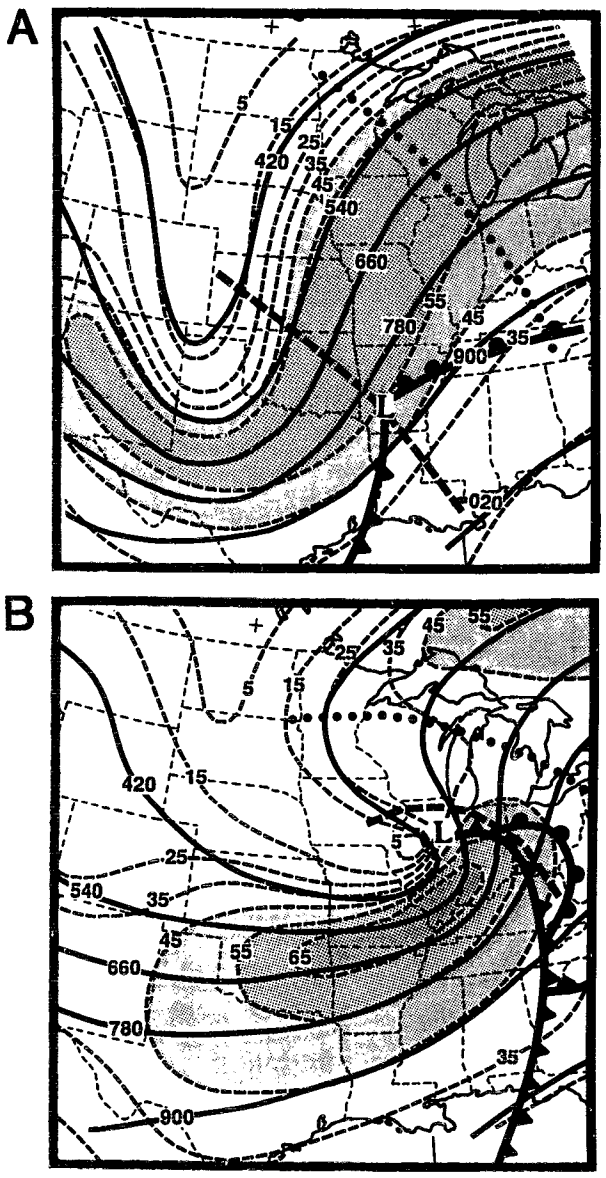

FIG. 22. Subjective analyses of 320-K isentropic surface (slopes from 250 mb northwest to 400 mb southeast). Montgomery streamfunction (solid, 540 = 3.540×10^5 m^2 s^{-2}) and isotachs (dashed; m s^{-1}) for (A) 0000 UTC and (B) 1200 UTC 15 December 1987. The position of the surface cyclone, surface fronts, 320-K ridge axis (dotted line), and 320-K inflection axis (dashed line) are also plotted.

framework, the gravity waves are initiated by geostrophic adjustment forced by low-level deformation of the baroclinic structure; in Uccellini and Koch (1987), the adjustment is forced by inertial-advective accelerations associated with an upper-level jet streak. Bosart and Sanders (1986) documented a close association between the genesis location of the large-amplitude mesoscale wave-disturbance and strong low-level frontogenesis northwest of an intense East Coast cyclone. On 15 December 1987, wave disturbance A was also closely associated with a synoptic-scale wind shift northwest of the intensifying Midwest cyclone (Fig. 9). However, this wind shift was not associated with a significant surface temperature gradient (e.g., RFD, Fig. 4b). Although evidence is inconclusive, the intensity of the thermal deformations and vertical circulations expected within this explosive cyclone, the agreement with Uccellini and Koch (1987), and the collocation of the waves with a cloud feature associated with strong positive vorticity advection indicate a potential role for geostrophic adjustment in wave generation and intensification for this case.

7. Forecasting and nowcasting guidelines

Given the uncertainties in analyses of these types of mesoscale wave events even in a case study mode, it should be obvious that forecasters face a formidable challenge in attempting to monitor gravity waves and to nowcast their impact on critical weather events. Although long-lived, large-amplitude mesoscale wave disturbances are not explicitly forecast by current operational numerical models, the conditions likely to result in their development might be anticipated using guidelines derived from studies of atmospheric gravity waves (Lindzen and Tung 1976; Uccellini and Koch 1987; Koch et al. 1988; Koch and Dorian 1988). The results of these studies suggest that significant long-lived mesoscale wave disturbances are most likely in areas where all of the following conditions are met simultaneously:

1) The area is located between the upper-level inflection and ridge axes, particularly when a significant jet streak is expected to approach the ridge axis. The northwestern boundary of the wave activity is usually delineated by the jet stream axis.

2) The area contains a stable layer beneath a layer of weak static stability (near dry adiabatic if unsaturated, or near moist adiabatic if near saturation). Stronger and deeper stable layers can typically support larger amplitude wave disturbances.

3) Above the stable layer, the area is characterized by weak dynamic stability (bulk $Ri < 1.0$) associated with strong vertical wind shear and weak static stability.

Fulfillment of these criteria does not guarantee the formation of long-lived mesoscale wave disturbances but does indicate an increased probability of their occurrence. Thus, whenever the synoptic environment is conducive to wave disturbance formation and maintenance, surface observations should be monitored for short-period pressure perturbations accompanied by a change in wind speed and/or direction but little change in surface temperature. The small temperature change criteria differentiates gravity wave disturbances from density currents or gust fronts. Many gust fronts can also be distinguished from gravity waves by the strong wind shift nearly coincident with the onset of a rapid pressure rise.

If similar pressure and wind fluctuations are observed at several other nearby stations, one can be fairly certain the weather is caused by a mesoscale wave disturbance.

Scrutiny of the SAs when wave activity is present should reveal special groups describing rapid pressure fluctuations or high wind gusts such as:

PRES UNSTDY (pressure unsteady),
LOWEST PRES (describes the magnitude and time of a pressure minimum),
PRJMP (describes the magnitude and time of a rapid pressure rise),
WSHFT (notes the time of an abrupt wind shift), and
PKWND (notes the magnitude and time of a strong wind gust).

Satellite and radar data may be useful in tracking wave disturbances. Mesoscale wave disturbances frequently cause development of a banded structure in the precipitation or cloud field and are directly responsible for the periodic nature of the precipitation (e.g., Uccellini 1975; Stobie et al. 1983; Koch et al. 1988). In the 15 December 1987 case, wave-trough A was associated with the leading edge of warm bands in IR satellite imagery and echo-free regions in radar data; whereas mesoscale pressure ridges were closely associated with bands of deep cold clouds and strong convective precipitation. When bands detected in satellite or radar data pass a nearby station, pressure and wind observations should be monitored to determine if the bands are in fact associated with atmospheric gravity wave activity (Fig. 3). However, the use of satellite or radar data to track the wave propagation is complicated by the fact that gravity waves which initiate deep convection sometimes remain coupled with the storms they trigger (Stobie et al. 1983; Einaudi et al. 1987; Koch et al. 1988), and at other times merely pass through the storms (Uccellini 1975; Koch et al. 1988).

Substantial variability in wave propagation velocities were revealed when the results of this study were combined with a cursory examination of 14 long-lived, large amplitude mesoscale wave disturbances documented by other investigators (Bosart and Cussen 1973; Eom 1975; Uccellini 1975; Stobie et al. 1983; Pecnick and Young 1984; Bosart and Sanders 1986; Bosart and Seimon 1988 (two waves); Ferretti et al. 1988; Savage et al. 1988; Lin and Goff 1988; Koch and Golus 1988; Ramamurthy et al. 1989 (two cases)). The directions of wave propagation for all of the cases examined were within a 90° arc rotating clockwise from the direction of the mid to upper-tropospheric wind direction. Reported propagation speeds varied between 10 m s^{-1} and 55 m s^{-1} (22 to 123 mph) with an average speed of about 28 m s^{-1} (62 mph).

At these propagation velocities, mesoscale wave disturbances can pass several stations within 1 h. New observing systems such as ASOS (Automated Surface Observing System) (Thompson 1986), NEXRAD (Next Generation Radar), and wind profilers (Golden et al. 1986) produce data with high temporal resolution that can be exploited with appropriate software to detect and track mesoscale wave disturbances. In the interim, forecasters must rely on timely and accurate wind, pressure and weather observations complete with special remarks. Routine documentation of mesoscale wave disturbance events will aid development of a more thorough synoptic climatology. When combined with insights from atmospheric gravity wave theory and output from numerical models, such a climatology could form the basis for skillful short-range forecasts of large-amplitude mesoscale wave disturbances and their influence on significant weather events.

8. Summary and discussion

This article documents the explosive cyclogenesis and dramatic gravity wave activity which occurred over the Midwest during the 15 h between 0000 UTC and 1500 UTC on 15 December 1987. Two particularly intense mesoscale wave disturbances are isolated using a combination of SA observations, surface barograms, and geostationary satellite imagery. The wave disturbances were first detected in Missouri and subsequently traversed a 400-km wide envelope extending northeastward to Michigan. Throughout most of their lifecycle, the two main wave disturbances were consistent with atmospheric gravity wave theory and were characterized by horizontal wavelengths between 100-km and 200-km, peak-to-peak pressure amplitudes of greater than 4 mb, and propagation velocities toward the north through northeast at approximately 30 m s^{-1} (62 kt).

Rapid changes in surface wind, pressure and precipitation rates associated with the wave disturbances made their detection and understanding essential to a successful short-range forecast on 15 December 1987. Wave disturbance passage was accompanied by pressure falls of up to 11 mb in 15 min, winds in excess of 25 m s^{-1}, cloud-to-ground lightning, and heavy snowfall. Although the cyclone-induced heavy snowfall was correctly forecast over northern Illinois and southern Wisconsin, unforecast wave-induced blizzard conditions complicated snow-removal operations and contributed to road and airport closures. Wave-induced alteration of the onset time of heavy snowfall also reduced the utility of synoptic-scale forecasts. In addition, wave-modified surface pressure and wind observations made it difficult to identify the location of the surface cyclone center and had the potential to cause inaccurate forecasts of its future motion. Basic guidelines based on the small-sample synoptic climatology by Uccellini and Koch (1987) and atmospheric gravity wave theory were detailed to help forecasters anticipate and identify mesoscale wave disturbances.

In addition to their extraordinary magnitude and associated weather conditions, the mesoscale wave disturbances were notable for their apparent interaction with the parent extratropical cyclone between 0800 UTC and 1000 UTC 15 December. The largest am-

plitude wave, characterized at the time by a surface pressure minimum lower than that of the cyclone, propagated through the cyclone center during the rapid intensification of the vortex (20 mb in 12 h). During interaction with the wave disturbance, the cyclone's central pressure fell 7 mb in 1 h followed by a 2-mb rise. The importance of this interaction to the explosive cyclogenesis is uncertain since accurate forecasts of cyclone intensification were attained by operational numerical models without simulation of the mesoscale wave disturbances.

Analysis of the wave disturbance environment revealed a close agreement with Lindzen and Tung's (1976) theory for an atmospheric wave duct which reduces vertical propagation of gravity wave energy and therefore permits long-lived waves. A deep low-level isothermal layer overlain by a conditionally unstable layer as required by the theory was observed at 0000 UTC 15 December over Missouri and Illinois. The conditionally unstable layer contained a critical level characterized by dynamically unstable vertical wind shears capable of generation and/or maintenance of gravity wave energy (Lindzen and Tung 1976; Stobie et al. 1983; Ferretti et al. 1988).

The processes responsible for the generation of the wave disturbances are less certain. The synoptic-scale environment on 15 December, characterized by a strong upper-tropospheric jet streak embedded in curved flow and approaching a ridge axis, was similar to a small-sample synoptic climatology for long-lived, large-amplitude mesoscale wave disturbances (Uccellini and Koch 1987). Uccellini and Koch use their climatology and atmospheric gravity wave theory to argue that mass-momentum imbalances near jet streaks are fundamental to formation of many large-amplitude wave disturbances. Agreement with this climatology and the close association of the 15 December wave disturbances with strong cyclonic vorticity advection ahead of an intense shortwave trough, suggest a potential role for shortwave-induced mass-momentum adjustment in wave disturbance generation. Convection may also have played a role in wave generation or amplification. The large-amplitude wave troughs were adjacent to bands of strong convection and therefore probably collocated with convectively induced subsidence zones. Although the presence of a dynamically unstable critical level was consistent with generation of large-amplitude, long-wavelength gravity waves through extraction of energy from the vertical wind shear of the environment (Stobie et al. 1983; Pecnick and Young 1984), the dynamic instability was apparently present over a broad region in space and time but the wave disturbances were localized.

The 15 December 1987 case illustrates that mesoscale wave disturbances, although infrequent, can have major impacts on local weather forecasts. The model characteristics and data coverage required for their accurate forecast or simulation within numerical models needs to be determined. There is also a need for comprehensive documentation of large-amplitude mesoscale wave events and concurrent development of a large-sample synoptic climatology which would aid development of large-scale probability forecasts of mesoscale wave disturbance activity. Finally, the relationship between the intense upper-tropospheric jet streak and shortwave, the large-amplitude mesoscale wave disturbances, and the rapid intensification of the surface cyclone should be explored. One focus should be the interaction between synoptic-scale forcing manifest as strong cyclonic vorticity advection and a mesoscale response manifest as large-amplitude wave disturbances.

Acknowledgments. The author is indebted to Stephen Jascourt for helping to initiate and improve this study and to Dr. Louis Uccellini for his continuous professional and scientific support. The author also extends warm thanks to Dr. Lance Bosart, Steve Silberberg, Charles Seman, and the anonymous reviewers for scientific exchanges and assistance which improved the manuscript. Figures were drafted by Cynthia Karls and Christine Johnson. The financial and scientific support of Professor Donald Johnson and the prompt response of numerous Weather Service offices to our initial data request are also gratefully acknowledged. This material is based upon work supported by the National Science Foundation under Grant ATM-8602860.

REFERENCES

Anderson, R. K., 1974: Application of meteorological satellite data in analysis and forecasting. ESSA Technical Report NESC 51. 330 pp. U.S. Department of Commerce, NESDIS, Available from the Superintendent of Documents, U.S. Government Printing Office, Washington, D.C. 20402 (AD-697-033).

Bosart, L. F., and J. P. Cussen, Jr., 1973: Gravity wave phenomena accompanying east coast cyclogenesis. *Mon. Wea. Rev.*, **101**, 446–454.

——, and F. Sanders, 1986: Mesoscale structure in the megalopolitan snowstorm of 11–12 February 1983. Part III: A large-amplitude gravity wave. *J. Atmos. Sci.*, **43**, 924–939.

——, and A. Seimon, 1988: A case study of an unusually intense atmospheric gravity wave. *Mon. Wea. Rev.*, **116**, 1857–1886.

Cahn, A., 1945: An investigation of the free oscillations of a simple current system. *J. Meteor.*, **2**, 113–119.

Carlson, T. N., 1980: Airflow through midlatitude cyclones and the comma cloud pattern. *Mon. Wea. Rev.*, **108**, 1498–1509.

Chimonas, G., and C. O. Hines, 1986: Doppler ducting of atmospheric gravity waves. *J. Geophys. Res.*, **91**, No. D1, 1219–1230.

Christie, D. R., K. J. Muirhead and A. L. Hales, 1978: On solitary waves in the atmosphere. *J. Atmos. Sci.*, **35**, 805–825.

——, 1989: Long nonlinear waves in the lower atmosphere. *J. Atmos. Sci.*, **46**, 1462–1491.

Doswell, C. A., 1982: Operational meteorology of convective weather. Volume I. Operational mesoanalysis. 164 pp. NOAA Technical Memorandum NWS NSSFC-5 (NTIS # PB83-162321).

Durran, D. R., 1986: Mountain waves. *Mesoscale Meteorology and Forecasting*, Ed., P. Ray, American Meteorological Society, 793 pp.

Einaudi, F., W. L. Clark, D. Fua, J. L. Green and T. E. VanZandt, 1987: Gravity waves and convection in Colorado during July 1983. *J. Atmos. Sci.*, **44**, 1534–1553.

Eom, J. K., 1975: Analysis of the internal gravity wave occurrence

of 19 April 1970 in the Midwest. *Mon. Wea. Rev.*, **103,** 217–226.

Fawcett, E. B., and H. K. Saylor, 1965: A study of the distribution of weather accompanying Colorado cyclogenesis. *Mon. Wea. Rev.*, 359–367.

Ferretti, R., F. Einaudi and L. W. Uccellini, 1988: Wave disturbances associated with the Red River Valley severe weather outbreak of 10–11 April 1979. *Meteor. Atmos. Phys.*, **39,** 132–168.

Fujita, T. T., 1955: Results of detailed synoptic studies of squall lines. *Tellus,* **4,** 405–436.

Fritts, D. C., 1984: Shear excitation of atmospheric gravity waves. Part II: Nonlinear radiation from a free shear layer. *J. Atmos. Sci.*, **41,** 524–537.

Golden, J. H., R. Serafin, V. Lally and J. Facundo, 1986: Atmospheric sounding systems. *Mesoscale Meteorology and Forecasting,* Ed., P. Ray, American Meteorological Society, 793 pp.

Goree, P. A., and R. J. Younkin, 1966: Synoptic climatology of heavy snowfall over the central and eastern United States. *Mon. Wea. Rev.*, **94,** 663–668.

Harms, R. W., 1973: Snow forecasting for southeastern Wisconsin. *Weatherwise,* **26,** p. 250.

Hooke, W. H., 1986: Gravity waves. *Mesoscale Meteorology and Forecasting,* Ed., P. Ray, American Meteorological Society, 793 pp.

Keyser, D., and M. A. Shapiro, 1986: A review of the structure and dynamics of upper-level frontal zones. *Mon. Wea. Rev.*, **114,** 452–499.

Koch, S. E., and P. J. Dorian, 1988: A mesoscale gravity wave event observed during CCOPE. Part III: Wave environment and probable source mechanisms. *Mon. Wea. Rev.*, **116,** 2570–2592.

——, and R. E. Golus, 1988: A mesoscale gravity wave event observed during CCOPE. Part I: Multiscale statistical analysis of wave characteristics. *Mon. Wea. Rev.*, **116,** 2527–2544.

——, —— and P. J. Dorian, 1988: A mesoscale gravity wave event observed during CCOPE. Part II: Interactions between mesoscale convective systems and the antecedent waves. *Mon. Wea. Rev.*, **116,** 2545–2569.

Ley, B. E., and W. R. Peltier, 1978: Wave generation and frontal collapse. *J. Atmos. Sci.*, **35,** 3–17.

Lin, Yuh-Lang, and R. C. Guff, 1988: A study of a mesoscale solitary wave originating near a region of deep convection. *J. Atmos. Sci.*, **45,** 194–205.

Lindzen, R. S., and K. K. Tung, 1976: Banded convective activity and ducted gravity waves. *Mon. Wea. Rev.*, **104,** 1602–1617.

Matsumoto, S., 1961: A note on geostrophic adjustment and gravity waves in the atmosphere. *J. Meteor. Res. Japan,* **39,** 18–28.

Pecnick, M. J., and J. A. Young, 1984: Mechanics of a strong subsynoptic gravity wave deduced from satellite and surface observations. *J. Atmos. Sci.*, **41,** 1850–1862.

Petterssen, S., 1956: *Weather Analysis and Forecasting.* Vol. 1. McGraw-Hill, 428 pp.

Ramamurthy, M. K., R. M. Rauber, B. P. Collins and P. C. Kennedy, 1989: Dramatic evidence of gravity wave induced precipitation bands: A twin case study. Preprints: *Twelveth Conf. on Weather Forecasting and Analysis,* Boston, Amer. Meteor. Soc., 537–542.

Rossby, C. G., 1938: On the mutual adjustment of pressure and velocity distributions in simple current systems, II. *J. Mar. Res.*, **1,** 239–263.

Sanders, F., 1955: An investigation of the structure and dynamics of an intense surface frontal zone. *J. Meteor.*, **12,** 542–552.

Savage, M. L., G. A. Weidner and C. R. Stearns, 1988: A diagnostic study of the influence of a gravity wave upon regional weather. *Mon. Wea. Rev.*, **116,** 347–357.

Shapiro, M. A., and P. J. Kennedy, 1981: Research aircraft measurements of jet stream geostrophic and ageostrophic winds. *J. Atmos. Sci.*, **38,** 2642–2652.

Skyllingstad, E. D., 1986: The effects of stratification and vertical wind shear on atmospheric solitary and cnoidal waves: A numerical investigation. Ph.D. dissertation, University of Wisconsin-Madison, 161 pp.

Stobie, J. G., F. Einaudi and L. W. Uccellini, 1983: A case study of gravity waves-convective storms interaction: 9 May 1979. *J. Atmos. Sci.*, **40,** 2804–2830.

Storm Data, 1987: U.S. Department of Commerce, National Climatic Data Center, Asheville, NC 28801, Vol. 29, No. 12.

Stull, R. B., 1988: *An Introduction to Boundary Layer Meteorology.* Kluwer Academic Publishers, 666 pp.

Suomi, V. E., R. Fox, S. S. Limaye and W. L. Smith, 1983: McIDAS III: A modern interactive data access and analysis system. *J. Climate Appl. Meteor.*, **22,** 766–778.

Tepper, M., 1951: On the desiccation of a cloud bank by a propagated pressure wave. *Mon. Wea. Rev.*, **79,** 61–70.

Thompson, D. W., 1986: Systems for measurements at the surface. *Mesoscale Meteorology and Forecasting,* Ed., P. Ray, Amer. Meteor. Soc., 793 pp.

Uccellini, L. W., 1975: A case study of apparent gravity wave initiation of severe convective storms. *Mon. Wea. Rev.*, **103,** 497–513.

——, and S. E. Koch, 1987: The synoptic setting and possible energy sources for mesoscale wave disturbances. *Mon. Wea. Rev.*, **115,** 721–729.

Young, J. A., and C. F. Richards, 1973: A climatological study of surface pressure events at Madison, Wisconsin: Preliminary results relating to possible gravity wave activity. Studies of the Atmosphere using Aerospace Probes, Space Science and Engineering Center 1973 Annual Report, University of Wisconsin-Madison, pp. 172–187. (NTIS # COM-74-11626/0.)